

# Vegetation and channel adjustment trajectories in cold regions: The effects of ice disturbances in two Gaspesian rivers

Matthieu Prugne<sup>1</sup>  | Dov Corenblit<sup>2</sup>  | Maxime Boivin<sup>3</sup>  | Thomas Buffin-Bélanger<sup>1</sup>

<sup>1</sup>Département de biologie, chimie et géographie, Université du Québec à Rimouski, Rimouski, Québec, Canada

<sup>2</sup>Paul Sabatier (UT3), Centre de Recherche sur la Biodiversité et l'Environnement (CRBE), Université de Toulouse, CNRS, IRD, Toulouse INP, Toulouse, France

<sup>3</sup>Laboratoire d'expertise et de recherche en géographie appliquée (LERGA), Université du Québec à Chicoutimi, Québec, Canada

## Funding information

Natural Sciences and Engineering Research Council of Canada, Grant/Award Number: RGPIN-2023-05431

## Abstract

Fluvial biogeomorphology has proven to be efficient in understanding the evolution of rivers in terms of vegetation succession and channel adjustment.

The role of floods as the primary disturbance regime factor has been widely studied, and our knowledge of their effects on vegetation and channel adjustment has grown significantly in the last two decades. However, cold rivers experiencing ice dynamics (e.g., ice jams and mechanical breakups) as an additional disturbance regime have not yet been studied within a biogeomorphological scope. This study investigated the long-term effects of ice dynamics on channel adjustments and vegetation trajectories in two rivers with different geomorphological behaviours, one laterally confined (Matapédia River) and one mobile (Petite-Cascapédia River), in Quebec, Canada. Using dendrochronological analysis, historical data and aerial photographs from 1963 to 2016, this study reconstructed ice jam chronologies, characterized flood regimes and analysed vegetation and channel changes through a photointerpretation approach. The main findings of this study indicate that geomorphological impacts of mechanical ice breakups are not significant at the decadal and reach scales and that they might not be the primary factors of long-term geomorphological control. However, results have shown that vegetation was more sensitive to ice dynamics. Reaches presenting frequent ice jams depicted high regression rates and turnovers even during years with very low floods, suggesting that ice dynamics significantly increase shear stress on plant patches. This study also highlights the high resiliency of both rivers to ice jam disturbances, with vegetation communities and channel forms recovering within a decade. With the uncertainties following the reach/corridor and decadal scales, future research should focus on long-term monitoring and refined spatial scales to better understand the mechanisms behind the complex interactions among ice dynamics, vegetation and hydrogeomorphological processes in cold rivers.

## KEYWORDS

riparian, vegetation, channel dynamics, dendrochronology, flow regime, fluvial landforms, hydrogeomorphic adjustments, ice-jams, riparian, succession, vegetation, vegetation succession

## 1 | INTRODUCTION

The hydrological regime is a key aspect that has been extensively researched to understand its role in the biogeomorphological dynamics of rivers. Geomorphological-oriented studies have explored how it

affects channel patterns and landform adjustments (Chen et al., 2019; Comiti et al., 2009; Dumitriu, 2020; Grams et al., 2020), while ecological-oriented studies have focused on vegetation richness and diversity (Jansson et al., 2005; Ochs et al., 2019; Steinberg et al., 2021) and succession trajectories (Garófano-Gómez et al., 2017;

This is an open access article under the terms of the [Creative Commons Attribution](https://creativecommons.org/licenses/by/4.0/) License, which permits use, distribution and reproduction in any medium, provided the original work is properly cited.

© 2025 The Author(s). *Earth Surface Processes and Landforms* published by John Wiley & Sons Ltd.

González et al., 2019; Surian et al., 2015). Frequency, amplitude, timing and duration of floods are known to act as the principal pulse disturbance that maintains the riverscape configuration and modulates the rate and intensity at which feedbacks occur between plants and fluvial processes (Corenblit, Steiger, Dufour, et al., 2024).

Many authors have successfully established relationships between hydrological disturbance regimes and biogeomorphological feedbacks within river systems (Bollati et al., 2014; Corenblit et al., 2020; Garófano-Gómez et al., 2022; Geerling et al., 2006; Lallias-Tacon et al., 2017; Scorpio & Comiti, 2024; Segura-Beltrán & Sanchis-Ibor, 2013; Serlet et al., 2018). Aerial photographs, satellite imagery and LiDAR mosaics have proven to be effective in qualitatively and quantitatively describing biogeomorphological feedback in the context of post-disturbance recovery (Mossa et al., 2020), ramp disturbances such as dam construction (Elder, 2003; Han et al., 2020), biogeomorphological construction of floodplains and in-channel morphologies (Corenblit et al., 2014; Geerling et al., 2006; Gurnell & Bertoldi, 2020) and cyclic dynamics of turnovers and recovery (Surian et al., 2015). Many regions of the world have been studied through this scope, and our knowledge of the biogeomorphological dynamic equilibrium modulated by a range of flood regimes and bioclimatic contexts has significantly increased (Corenblit, Piégay, Arrignon, González-Sargas, Bonis, Davies, et al., 2024; Corenblit, Piégay, Arrignon, González-Sargas, Bonis, Ebengo, et al., 2024; Corenblit, Steiger, Dufour, et al., 2024). However, rivers in cold-temperate and cold regions experiencing river ice dynamics as an additional disturbance regime have yet to be approached within a biogeomorphological scope.

River ice dynamics have been shown to act as major morphogenic and ecological agents in northern rivers through many processes and ice forms, such as low temperatures, short growing seasons, frequent freeze–thaw cycles, riparian ice and anchor ice (Chassiot et al., 2020; Engström et al., 2011; Ettema & Kempema, 2012; Karle, 2003; Kimiaghali et al., 2015; Lind & Nilsson, 2015; Turcotte et al., 2011; Yumoto et al., 2006). The most impactful and studied processes are linked to mechanical ice breakup (i.e., physical disintegration of river ice due to thermal expansion, water flow and mechanical forces), which causes an important quantity of ice blocks to be transported downstream. These ice blocks are of various sizes, and their associated shear forces are known to directly erode vegetation and sediment or indirectly reduce bank resistance to flood by exposing root systems (Beltaos & Burrell, 2021; Vandermause et al., 2021); however, the magnitude of these impacts is known to be modulated by the type of vegetation and breakup intensity at a given site (Karle, 2007; Poulin et al., 2019; Rood et al., 2007). Furthermore, ice blocks can accumulate when their movements are restrained by geomorphological or anthropic features, such as meanders or bridges, eventually causing ice jams (Boucher, 2017; De Munck et al., 2017). Ice jam formation and release have been repeatedly shown to affect channel planforms and vegetation through scouring (Boucher et al., 2009; Prowse & Culp, 2003; Uunila & Church, 2014), flooding (Kovachis et al., 2017; Livingston et al., 2009; Peters et al., 2016) and avulsions (Boivin et al., 2017; Jones & Schumm, 1999; Kramer & Wohl, 2014; Smith et al., 1989; Smith & Pearce, 2002). Many impacts of mechanical breakups and ice jams have been studied but there is a lack of knowledge on the medium-term to long-term effect on river decennial evolution and its role on the biogeomorphological equilibrium related to changes in channel and riparian vegetation patterns.

The main objective of this study was to analyse the adjustment trajectories of riparian vegetation and channel patterns in the context of mechanical ice breakups at the fluvial corridor and multidecadal scales. Two contrasting rivers were selected for the study, one laterally confined and one unconfined, to assess the differences in response to ice dynamics in contrasting geomorphological behaviours. The specific objectives of this study are to (1) reconstruct the ice jam chronologies from dendrochronological analysis along with historical data and analyse the flood regime to characterize the disturbance regime in both rivers, (2) analyse both vegetation and channel trajectories from historical series of aerial photographs through photointerpretation to identify patterns related to the effects of disturbance regimes and (3) assess the possibility of detecting significant impacts of ice dynamics on the biogeomorphological adjustment and recover processes in both study rivers.

## 2 | METHODOLOGY

### 2.1 | Study rivers

The Matapédia and the Petite-Cascapédia Rivers located within the Gaspesian Peninsula in Quebec, Canada, were selected for this study (Figure 1A). They share similarities according to their sedimentary structure and vegetation but they expose significant differences in their mobility. Both rivers are mountainous gravel-bed rivers, located in a cold-temperate/boreal bioclimatic domain in the presence of mixed stands of balsam poplar (*Populus balsamifera* L.), balsam fir (*Abies balsamea* [L.] Mill., 1768) and black spruce (*Picea mariana* [Mill.] BSP., 1888). Both are characterized by a nivo-pluvial flood regime with two periods of high discharges, one caused by snowmelt in the Spring and one caused by intense rains in the Autumn. The Matapédia River has virtually no mobility due to confinement by rock outcrops and rip rap to protect a road and railway line parallel to the river, while the Petite-Cascapédia River shows high lateral mobility and numerous avulsions. The combination of these similarities and differences offers an opportunity to analyse the impact of ice dynamics on two contrasting rivers.

The Matapédia River originates from Lake Matapédia and flows north–south into the Restigouche River. Its watershed has an area of approximately 3,792 km<sup>2</sup>, with daily flow discharge ranging between 5 and 940 m<sup>3</sup>s<sup>-1</sup>, respectively. The mean annual flow is estimated to be approximately 56 m<sup>3</sup>s<sup>-1</sup> and the bankfull discharge is estimated at 414 m<sup>3</sup>s<sup>-1</sup>. The Matapédia River is frequently disturbed by important ice jams that cause major infrastructure damage, which has led to historical documentation about the year and location of different ice jams (Beltaos & Burrell, 2010). The study reach represents the downstream 33 km of the river from Routhierville municipality to the Matapédia municipality at the confluence with the Restigouche River (Figure 1B), with a confinement index  $\left(\frac{\text{Channel width}}{\text{Valley width}}\right)$  around 0.65.

The Petite-Cascapédia River originates in the mountains of Gaspésie Park and flows north–south into Chaleur Bay. Its watershed's area is about 1,449 km<sup>2</sup>, less than half of Matapédia's watershed area, and its daily flow discharge ranges between 3 and 623 m<sup>3</sup>s<sup>-1</sup>, with a mean annual discharge of 31 m<sup>3</sup>s<sup>-1</sup>. The Petite-Cascapédia presents evidence of ice jams through ice-scarred trees, but very little historical data are available. It is a highly mobile river with a confinement index  $\left(\frac{\text{Channel width}}{\text{Valley width}}\right)$  around 0.12, with high rates of

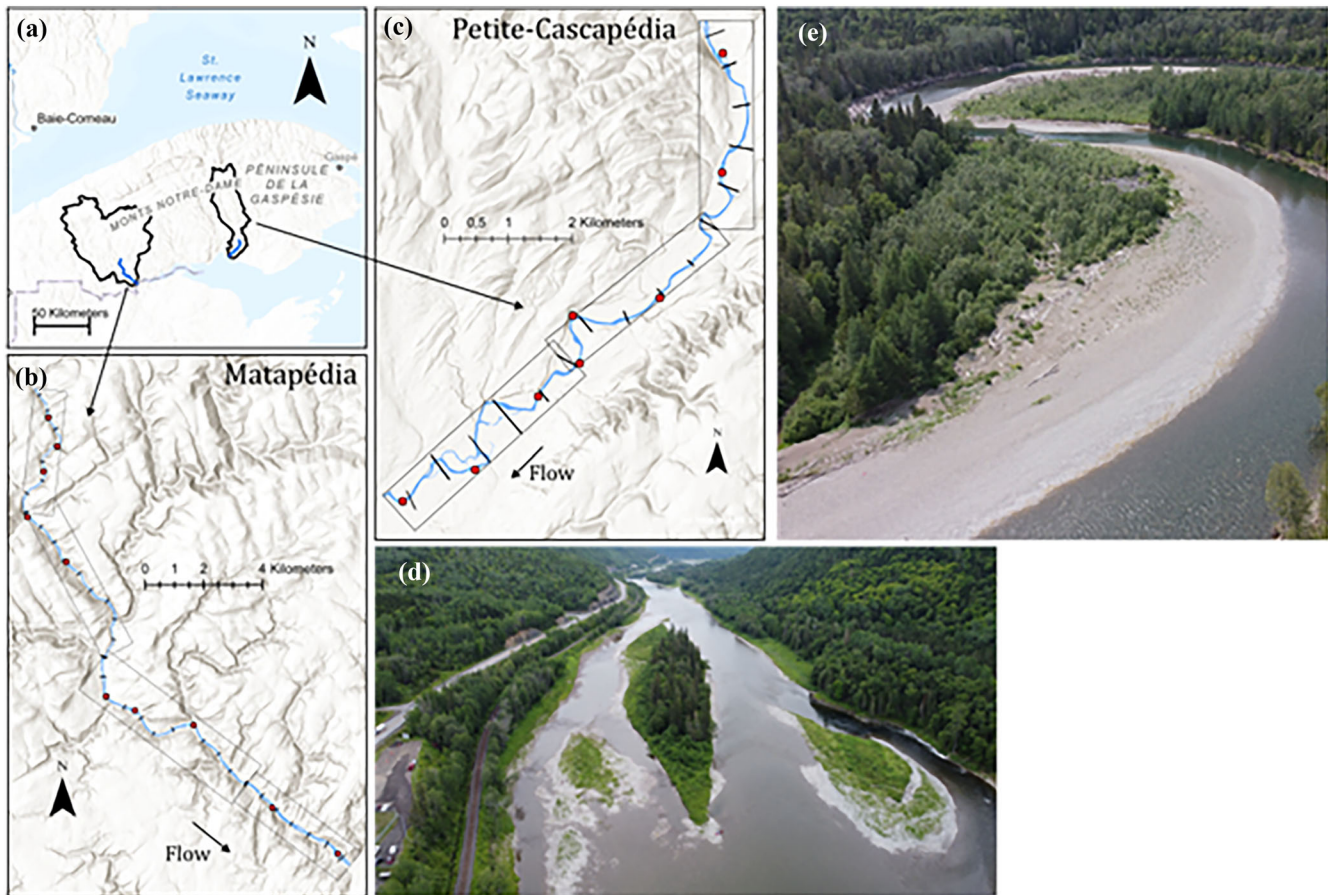


**FIGURE 1** Figure of the study sites. (A) Location map of the two watersheds on the Gaspesian Peninsula, Canada. (B and C) Map of the studied river segments (B for Matapédia River and C for Petite-Cascapédia River); blue polygon represents the active channel, black squared outlines the study reaches, black lines along the channel represent the limits of the 1 km subreaches and red points identify the dendrochronological sampling sites. (D and E) Oblique photographs (camera angled between 30 and 60 degrees from vertical) of the Matapédia River (D) and the Petite-Cascapédia River (E).

lateral migration and many avulsions that have occurred in recent decades. The study area consists of a section approximately 16 km upstream of the municipality of New Richmond (Figure 1C).

## 2.2 | GIS imagery

This study was based on a diachronic analysis of aerial photographs from 1963 to 2016. Sets of photographs covering both rivers were georeferenced based on a 2016 orthomosaic from the MELCCFP (*Ministère Environnement et Lutte aux Changements Climatiques et Forêts et Parcs*) with anthropic (e.g., roads and buildings) and natural (e.g., cut-off channel and deciduous trees patch) control points the closest to the channel as possible. Table 1 summarizes the scale of the photographs, mean RMSE from the georeferencing process and mean and maximum discharges at the time the pictures were taken.

## 2.3 | Characterization of ice jam and flood chronologies

A chronology of ice jam disturbances was constructed using historical and dendrochronological sources. For each river, historical local newspapers from 1950 and later were searched through the BanQ

(*Bibliothèque et archives nationales du Québec*) to find articles assessing the presence of impactful ice jams that occurred along the rivers, with which we identified the year of the event and its approximate location. Supplementary information was obtained from the local watershed organization OBVMR (*Organisme de bassin versant Matapédia-Restigouche*) and the MSP (*Ministère de la Sécurité du Québec*), who kept records of ice jams for the last couple of decades. Finally, a dendrochronological analysis of ice-scarred trees was performed to identify the location and years of ice jams (Lubiniecki et al., 2024; Taylor, 2009), as well as the height above the bankfull level of the scar. For both rivers, 200 tree cross-sections and wedges were collected from 18 different sites (Figure 1B-C). At each site, which was approximately 200 m long, samples were only taken from trees with visible scars. Samples were brought to the laboratory to be sanded and rings were counted, for which the latest ring was assumed to have grown in 2022. To avoid isolated events that could be misinterpreted as ice jams (e.g., impacts from large woody debris), we (1) took samples at a site only when multiple trees presented scars at the same height, assuring it came from mechanical breakups, and (2) considered ice jam years as confirmed only when a dated year was present in at least two different samples (Figure 2C).

On the Matapédia river, water gauge stations 011507 (48°5'19.00"N, -67°6'2.02"W) and 011509 (48°6'28.40"N, -67°7'48.79"W) were used to analyse flow discharge time series with

**TABLE 1** Aerial photographs and their characteristics used to analyse planform and vegetation trajectories.

Year	Photo type	Scale/resolution	Mean RMSE (m)	Mean Q (m <sup>3</sup> s <sup>-1</sup> )	
Matapédia					
1963	BW photographs	1:15,840	3.92	-	-
1975	BW photographs	1:15,000	2.79	21	67
1985	INF photographs	1:15,000	3.89	28	42
1993	INF photographs	1:15,000	3.48	41	52
2004	INF + BW photographs	1:15,000	2.69	61	406
2016	RGB Orthomosaic	0.3 m	-	25	-
Petite-Cascapédia					
1963	BW photographs	1:15,840	3.04	24	41
1975	BW photographs	1:15,000	-	16	22
1986	INF photographs	1:15,000	3.72	11	12
1992	INF photographs	1:15,000	3.72	22	31
2004	BW photographs	1:15,000	3.71	90	207
2016	RGB Orthomosaic	0.3 m	-	14	-

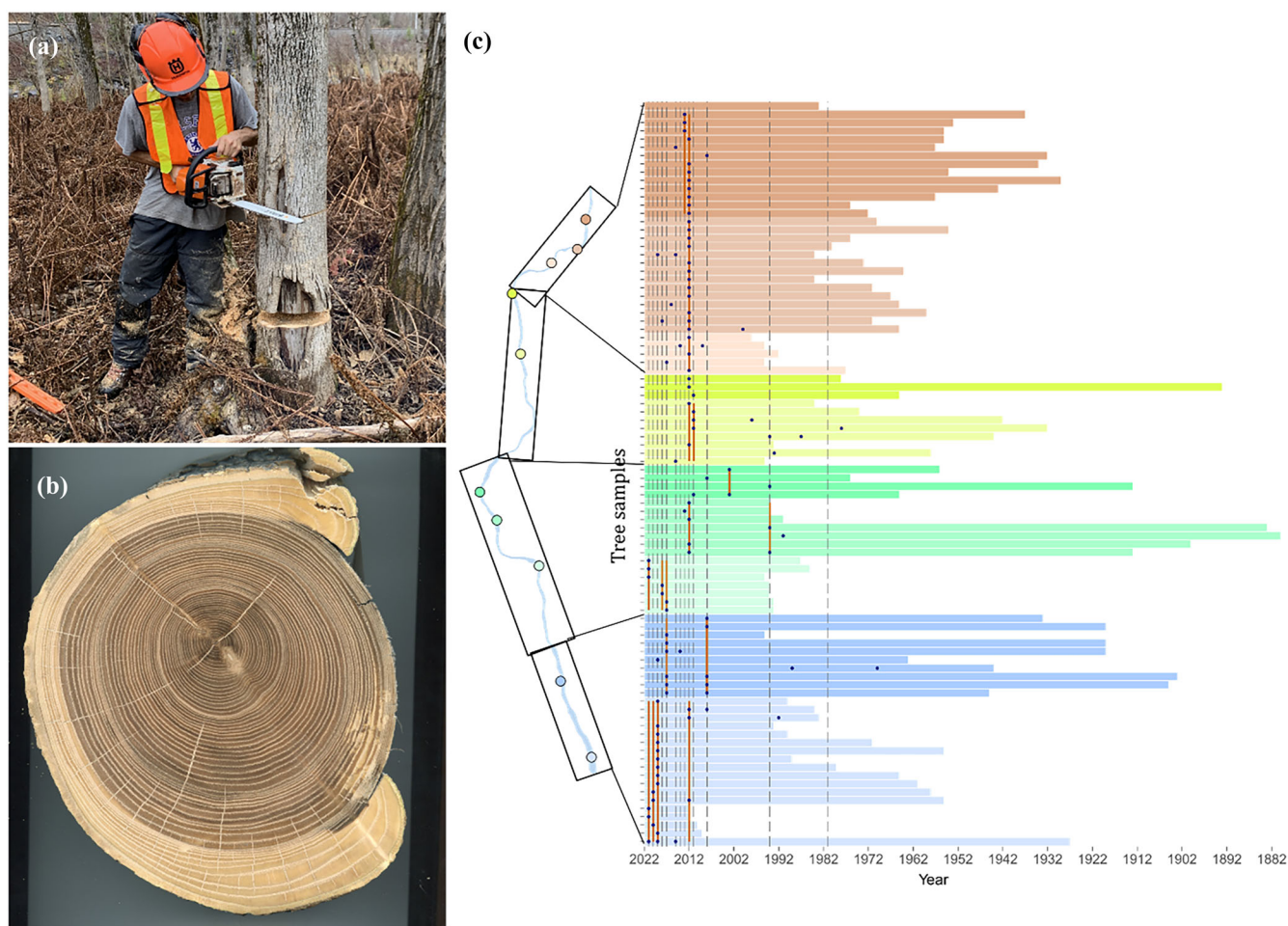


**FIGURE 2** (A) Picture of the sampling method: cutting of wedges at two different identified scars. (B) Example of a scanned tree cross-section with visible ice scars forming a “cat’s paw”. (C) Graph showing results from dendrochronological analysis; tree samples are on the ordinate and dating year on the abscissa; coloured bars (colours are according to river reach and tones to sampling sites) show the maximum rings counted for each sample, dark blue points indicate the dated ice jams events and orange bars indicate the confirmed ice jams with respect to the rule of  $n > 2$ .

available data from 1968 to 2023. On the Petite-Cascapédia River, the water gauge stations were the 010902 (48°13′55.70″N, –65°43′59.02″W), 010903 (48°13′55.99″N, –65°44′2.22″W) and

010901 (corrected data; 48°11′26.89″N, –65°48′38.6″W) with available data from 1963 to 2023. All the data came from the CEQ (*Centre d’expertise Hydrique du Québec*) database. Flood recurrence intervals

of 2, 5, 10, 20 and 50 years were calculated using the Weibull formula for each river and the number of floods was counted for each period. Each flood recurrence interval are annotated as  $Q_2$ ,  $Q_5$ ,  $Q_{10}$ ,  $Q_{20}$  and  $Q_{50}$ . As the water gauge stations missed some recordings, the following years were discarded: 1993 for the Matapédia River and from 2006 to 2009 for the Petite-Cascapédia River. Important floods that occurred on the Petite-Cascapédia River damaged the water gauge stations and biased the time series. To fill this gap, we used estimated discharges calculated by Buffin-Belanger et al. (2022) in a report submitted to the MAMH (*Ministère des Affaires Municipales et de l'Habitation*, government of Quebec).

## 2.4 | Analysis of geomorphological trajectories

To analyse the geomorphological adjustments and trajectories of both rivers, the active channel was photointerpreted and digitized for each decade on aerial photographs. The active channel was considered as the wetted part of the channel, including the unvegetated bars within the channel, estimating the area entirely covered by water for 2 years recurrence floods. The valley bottom was also traced to subdivide the study area into 1 km subreaches along the river (Figure 1). From these polygons, we calculated the channel width, lateral migration rate and erosion-deposition rate at the subreach, reach and river corridor scales. The channel width was measured as the ratio of the active channel area ( $A$ ) to the thalweg length ( $L$ ), by averaging the width of the active channel at a given scale. Lateral migration was measured using the Aggregated Migration rate index (AMI) from Jautzy et al. (2022), and the erosion and deposition areas were measured from the difference between active channel polygons of different years. Each planform change was further standardized to reflect the percentage of either the average channel width (i.e., width and lateral migration) or the average channel area (i.e., erosion and deposition). This standardization is useful because it enables the comparison of geomorphological changes across areas of varying sizes, ensuring that changes are proportionally represented relative to the channel dimensions. Finally, the sinuosity index was calculated for each year in each reach by dividing the channel thalweg length by the shortest straight line passing through each reach.

## 2.5 | Analysis of vegetation succession processes

Adjustments of vegetation and succession trajectories were assessed based on the photointerpretation of six land cover classes (water bodies, bare surface, sparse vegetation, dense vegetation, forest and anthropogenic) at the valley bottom to further identify the in-channel effect of ice and the potential ice-flood effect in the floodplain. These classes were chosen based on their generic characteristics. Differences in the angle and quality between the two photographs could make the differentiation between tall herbs and small shrubs quite difficult. By obtaining these large classes, we can reduce the photointerpretation error. Table 2 summarizes the principal descriptions and characteristics of each class and specifies the choices made.

Polygons of classes were compared from year to year at both the reach and sub-reach scales. For each subsequent pair of years (e.g., 1963–1974), the classified vectors were intersected to extract

**TABLE 2** Description of each surface cover and their visual characteristics used for photointerpretation.

Classes	Description	Visual characteristics
Water bodies (WA)	Area covered by water, both in the principal, cut off and abandoned channels.	Dark or bluish tint with homogeneous texture for each emulsion.
Bare surface (BS)	Composed principally of accumulation bars, the bare surface represents every area where no vegetation (0%) is present, representing high hydrological influences.	White or beige, these substrates were identified with light tint and homogeneous fine texture for each emulsion.
Sparse vegetation (SV)	Composed of areas where low vegetation starts to colonize. Principally present on accumulation bars, it represents areas where fluvial processes dominate the vegetation dynamic and where the habitats seem unstable.	Areas where vegetation can cover from 10% to 80% of bare substrate. Vegetation colour varied between types of emulsions (red for infrared, dark grey for B&W and green for RGB) but they all showed similar grain effects produced by the contrast between bare substrate and vegetation.
Dense vegetation (DV)	Dense vegetation represents a large range of dense pioneer vegetation that seems stable. It comprises every community of tall and dense herbs, shrubs and young trees communities.	Areas where vegetation cover is 100%. Depending on the type of communities, it could range from homogeneous and smooth texture to light textured caused by shrubs of low tree canopy.
Forest (FO)	Represents post-pioneer mature forest without distinction between coniferous or deciduous trees.	Highly textured produced from canopy cover. Large shadows near the canopy.
Anthropogenic (ANT)	This class encompasses all surfaces that are affected by human actions, including agricultural land, unnatural pasture and meadows, deforestation, riprap banks and inhabited spaces.	Agriculture, pasture and meadow lands were identified from a highly homogeneous low vegetation with unnatural patch shape (e.g., perfect rectangle).

new polygons assessing the trajectory of change from one class to another (e.g., SV to DV). The categories of change were then aggregated into the following groups: progression, regression and stability. For the analysis of natural changes, changes from and going to the anthropogenic class were excluded from the analysis.

Indices were used to characterize the trajectory of change based on the proportion of the total area that experienced changes. The indices followed the equation  $I_{abc} = \frac{\text{Progression} - \text{Regression}}{\text{Progression} + \text{Regression} + \text{Stable}}$ , where *progression* is the area for which the initial phase changed to a later state

of development, *regression* is the area for which the initial phase change to a earlier state of development, and *stable* is the area for which the initial phase did not change. It is important to note that these terms are used here as a simplified framework to describe the net trajectory of change between two specific years. We acknowledge that the actual dynamics of vegetation in riverine environments are often non-linear and may involve multiple intermediate states; thus, the progression–regression model should be viewed as an integrative

**TABLE 3** Change classes used to calculate the different indices. For example, the progression value for  $I_{BS}$  came from the sum of BS-SV (bare surface to sparse vegetation), BS-DV (bare surface to dense vegetation) and BS-FO (bare surface to forest).

Index	Progression	Regression	Stable
$I_{BS}$	BS-- > SV BS-- > DV BS-- > FO	BS-- > WA	BS-- > BS
$I_{SV}$	SV-- > DV SV-- > FO	SV-- > BS SV-- > WA	SV-- > SV
$I_{DV}$	DV-- > FO	DV-- > SV DV-- > BS DV-- > WA	DV-- > DV
$I_{FO}$	-	FO-- > DV FO-- > SV FO-- > BS FO-- > WA	FO-- > FO
$I_{all}$	All of the above	All of the above	All of the above

summary rather than a detailed account of all temporal pathways. The sign of the resulting index corresponds to the dominant process (positive for progression or negative for regression), and the value ranging from  $-1$  to  $1$  represents the importance of the dominant process. The closer the number is to  $-1$  or  $1$ , the more important the proportion of change is, and an index of  $0$  means that there is no dominant process. This index was applied to the overall change dynamics ( $I_{all}$ ) and for each cover type (Table 3).

## 3 | RESULTS

### 3.1 | Disturbance regime

Dendrochronological results depict a clear increase in ice-jam frequencies for both the Matapédia and Petite-Cascapédia rivers, where events were recorded almost annually as of 2008 (Figure 3). However, the confirmed ice jam showed high spatial variation. Jams rarely happen on the entire rivers' length. Instead, these events were localized, except for 2012 in the Matapédia River, where ice jams were confirmed at 7 out of 10 sites.

While ice jams were more frequent post-2008, the average height of the scars was lower than that of the oldest ice-jam years, suggesting a moderate ice-jam magnitude or potential channel incision, which lowered the riverbed. The highest magnitude jams occurred in 1994, with scars more than 2 m above the bankfull level. In fact, 1994 has been largely documented as it caused severe damage

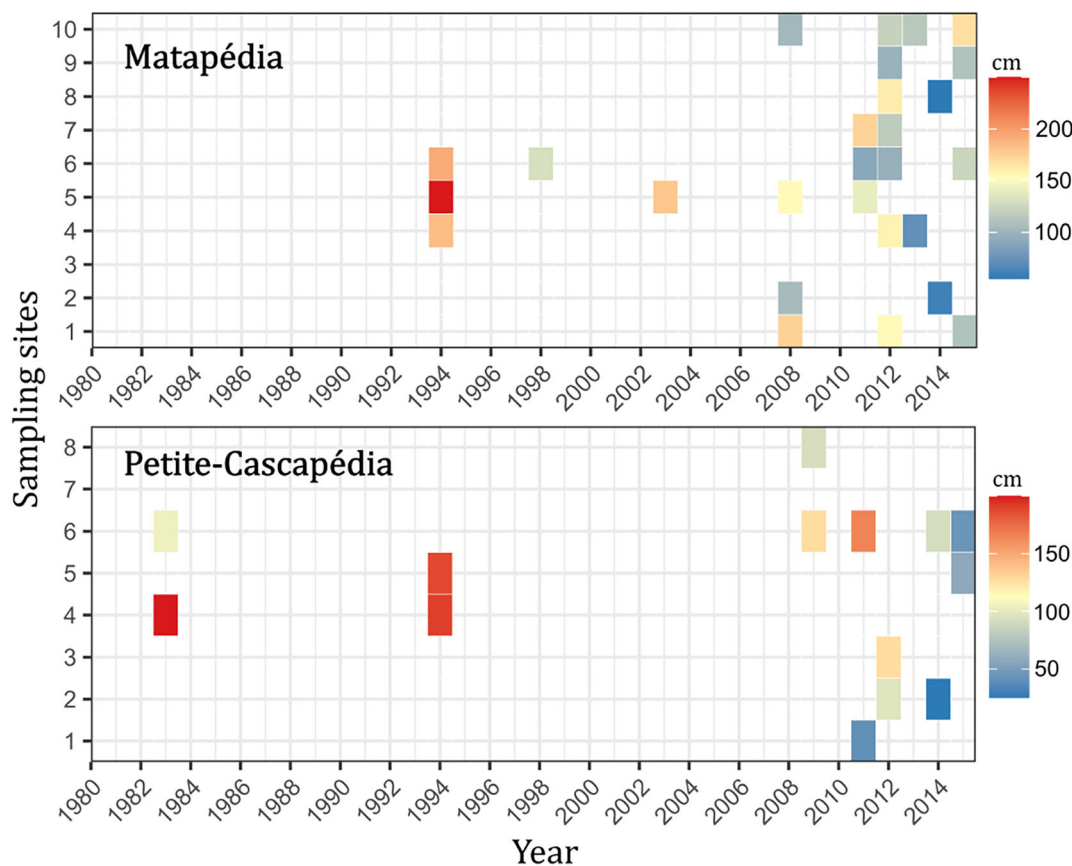


**FIGURE 3** Site locations and dated years of confirmed ice jams. Y-axis represents the site number along the rivers in which the identified ice-jam happened and x-axis represents the dated years. The colour gradients correspond to the average height (cm) of the scars above the bankfull level.

to anthropic structures along the Matapédia River. Additionally, the magnitude of jams seems to be highly variable from site to site when considering the average scar height within a site, ranging from 92 to 181 cm in the Matapédia River and from 40 to 199 cm in the Petite-Cascapédia River (Table S1).

With trees being uprooted during high floods or severe mechanical ice breakups, we must consider the possibility of missing years in the dendrochronological analysis. However, historical data of ice jam records helped to confirm five additional years (1974, 1983, 1984, 1995 and 2009) in the Matapédia River and one more year (2015) in the Petite-Cascapédia River (Table 4).

The merged historical and dendrochronologically confirmed ice jam years were overlaid onto the discharge time series to display temporal trends in the magnitude and frequency of floods and jams (Figure 4). In the Matapédia River, the highest daily maximum discharge was  $940 \text{ m}^3\text{s}^{-1}$  in 1979, which corresponds to a flood recurrence interval of more than 50 years. The period of 1974–1985 was the most flood-impacted period, with  $Q_{50}$  ( $730 \text{ m}^3\text{s}^{-1}$ ) attained once,  $Q_{10}$  ( $550 \text{ m}^3\text{s}^{-1}$ ) attained twice, and  $Q_5$  ( $496 \text{ m}^3\text{s}^{-1}$ ) attained four times (Table S2). On the other hand, the period of 1993–2004 was the lowest flood-disturbed period with only an  $Q_2$  frequency of 0.4, meaning that more than half of this period was impacted by floods below the bankfull level. The highest recorded discharge on the Petite-Cascapédia River was  $700 \text{ m}^3\text{s}^{-1}$  in 2011, corresponding to a flood recurrence of 50 years. The period of 2004–2016 was the most

affected period by flood, with one flood of  $Q_{50}$ , two floods of  $Q_{10}$  ( $600 \text{ m}^3\text{s}^{-1}$ ), and six floods of  $Q_2$  ( $275 \text{ m}^3\text{s}^{-1}$ ). The period of 1986–1992 was the least disturbed in the study, with only three floods that attained the water level of  $Q_2$ .

Figure 5 summarizes the trends in the flood discharge and ice jam regimes over time (Figure 5A) and space (Figure 5B). For both rivers, the number of ice jams has increased over time. This trend is particularly evident for the Matapédia River, where the number of ice jams constantly increased from 1963 to 2016, except for the period of 1985–1993 where no ice jams were recorded. However, flood regime trends differed in both rivers. Matapédia depicts a marginal decrease in the mean peak discharge, from approximately  $500 \text{ m}^3\text{s}^{-1}$  to  $400 \text{ m}^3\text{s}^{-1}$ , with the lowest point in the period of 1993–2004. Conversely, the Petite-Cascapédia shows a significant increase with a mean peak discharge passing from  $249 \text{ m}^3\text{s}^{-1}$  to  $392 \text{ m}^3\text{s}^{-1}$ , with the lowest mean peak discharge in the period 1986–1986. While the discharge data can only be used at the river scale, we can spatialize the ice regime along the predefined reaches (Figure 5B). In the Matapédia River, the most downstream reach (1) was where the highest number of ice jams was recorded during the entire study period. In the Petite-Cascapédia River, the highest number of identified ice jams was in the middle reach (2).

### 3.2 | Geomorphological planform adjustments

Geomorphological adjustments were assessed through the trajectory of change according to the river width, lateral migration and erosion/deposition rate. The results were standardized to represent the changes as the proportion (%) of the average river width per subreach for the width change and lateral migration and as the proportion (%) of the average channel area per subreach for the erosion/deposition rate. Table S3 summarizes the average width and area of the sub-reaches to scale the results presented in this subsection. Matapédia and Petite-cascapédia are two contrasting rivers in terms of width and mobility (Figure 6). The downstream section of the Matapédia River (first 18 km) has an average channel width of 110 m while the upstream section's mean width is approximately 70 m. The Petite-Cascapédia channel averages a smaller width of 74 m but presented more variability over time (Figure 6B).

In Matapédia, the sinuosity index showed no significant changes over the years, bar surface areas significantly dropped in 2004 but were similar across the other dates, and width variation was marginal, except for reach 1, where the channel was narrowed by 14 m in 2004 (Figure 7). Petite-Cascapédia showed higher sinuosity across all reaches and higher bar surface dynamics. The highest sinuosity variation occurred in reach 1, with a maximum of 1.42 attained in 2004 before dropping back to 1.37, while the bar surface areas presented high cyclical dynamics from year to year. While widths were smaller in the Petite-Cascapédia, their variations were more pronounced, especially in reach one, where it varied between 94 and 78 m.

The average width change rate in the Matapédia River ranged between 0.1%/yr and 0.2%/yr for the narrowing and enlargement processes (Figure 8A). Although most width changes in Matapédia were insignificant, some trends were evident. Narrowing dominated except for 1985–1993, where enlargement was prevalent. The rate of change varied across the sub-reaches. The highest narrowing rate was

**TABLE 4** Years in which ice jams occurred based on dendrochronological analysis, historical newspapers, watershed organizations databases and government databases and reaches in which they occurred.

Year	Dendro	Newspaper	OBVMR	MSP	Reach
<b>Matapédia</b>					
1974		x	x		1
1983		x			1
1984		x			1
1994	x	x	x	x	1, 2, 3
1995		x			1, 2
1998	x				3
2003	x				2
2008	x				1, 2, 4
2009		x		x	1
2011	x			x	1, 2, 3
2012	x				1, 2, 3, 4
2013	x				2, 4
2014	x	x	x	x	1, 4
2015	x			x	1, 3, 4
<b>Petite-Cascapédia</b>					
1983	x				2
1994	x			x	2
2009	x				2, 3
2011	x				1, 2
2012	x				1
2014	x				1, 2
2015				x	2

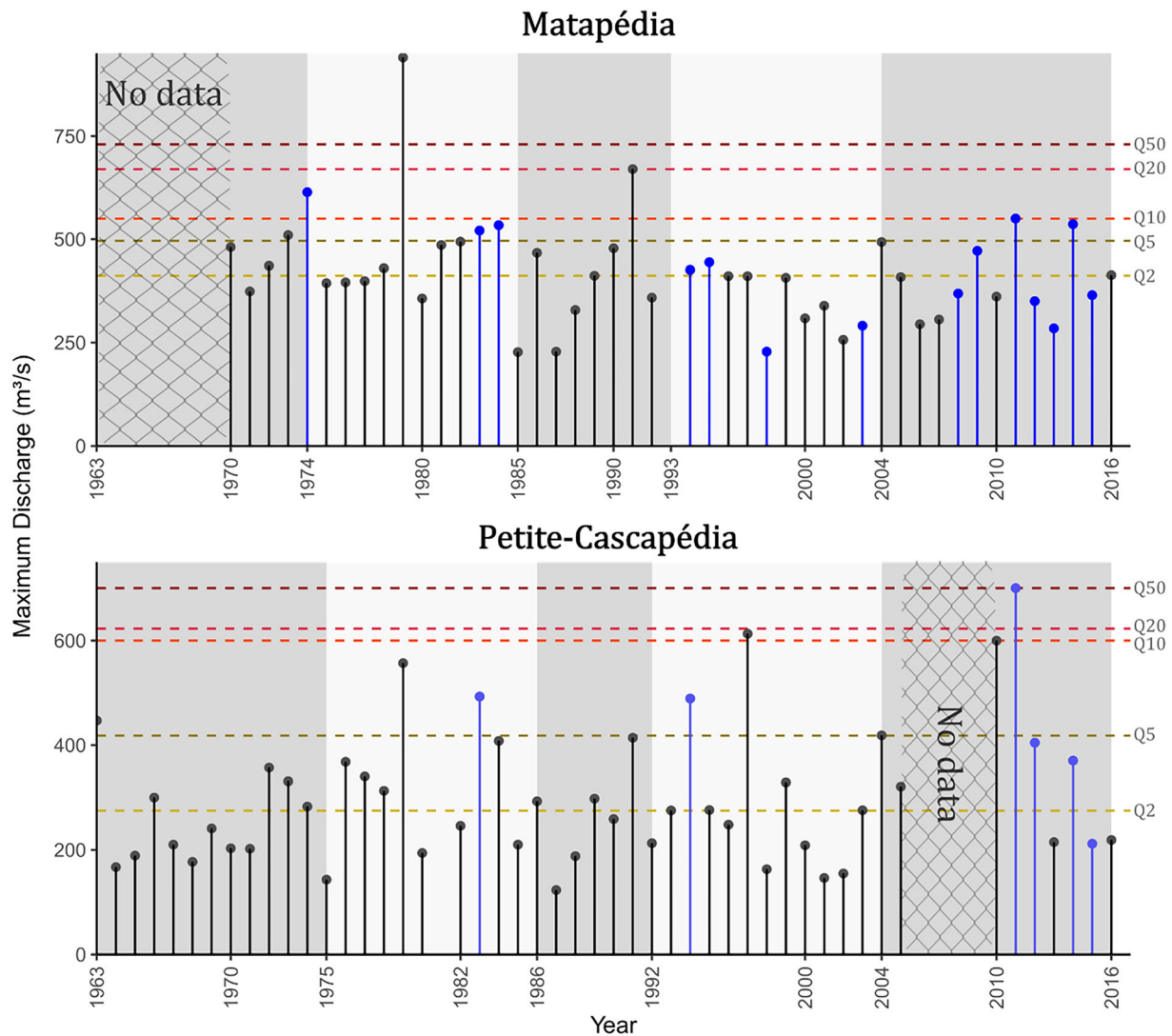


**FIGURE 4** Time series of available maximum discharges for both rivers. The coloured horizontal lines represent the discharges associated with flood recurrences  $Q_2$ ,  $Q_5$ ,  $Q_{10}$ ,  $Q_{20}$  and  $Q_{50}$ . The blue points and vertical lines represent the years with known ice jam events. The alternating grey and white colours show the periods between the available series of aerial photographs. The hatched areas identify missing data of flood discharges.

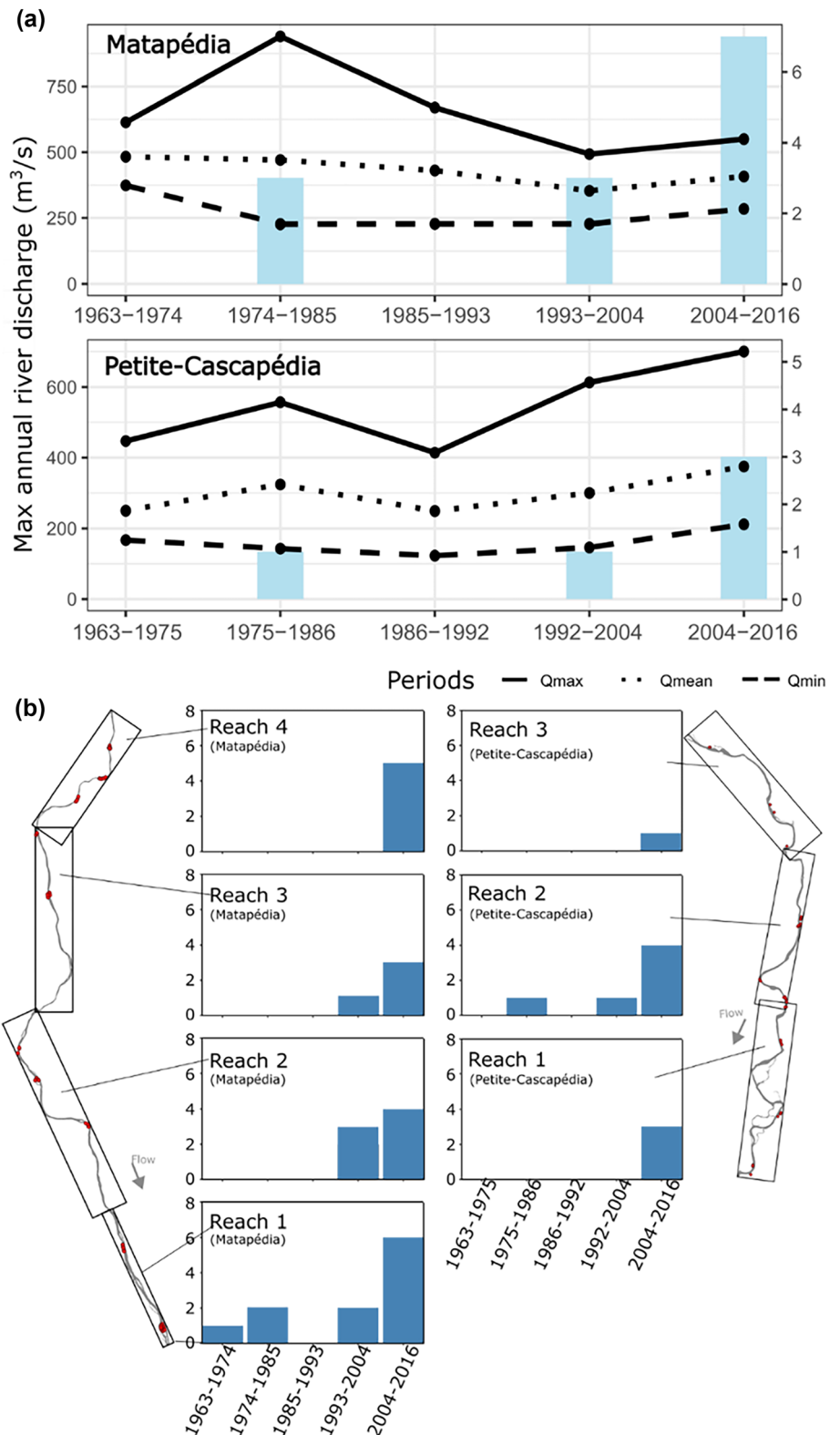
2.4%/yr at subreach 1 (1985–1993), which narrowed by almost 30 m. While reach 4 was measured as a high enlargement rate in 1993–2004 (1.5%/yr) and a high narrowing rate in 2004–2016 (1.5%/yr), these are the biases from the high flood of  $400 \text{ m}^3\text{s}^{-1}$  that occurred while the 2004 photograph was taken. The Petite-Cascapédia River showed higher rates of change with alternating narrowing and enlargement (Figure 8A). The highest narrowing rates were 0.9%/yr and 0.5%/yr during the period of 1963–1975 and 1986–1992, respectively. These were interspersed with increasing rates of 0.7 and 0.1%/yr during 1975–1986 and 1992–2004.

The inter-reach average mean width change rates showed temporal trends (Figure 8B). In Matapédia, each reach responded differently to the survey. Reach 3 and 4 had the highest enlargement rates (0.18 and 0.4%/yr) in 1985–1993. Reach 1 generally narrowed from 1963 to 2004, and then enlarged from 2004 to 2016. Reach 2 remained stable with minimal narrowing (0.15%/yr). The changes in the Matapédia River are marginal compared to those of the Petite-Cascapédia River, which show significant changes between  $-1.5$  to 1.5%/yr. Reaches 1 and 3 alternated between narrowing and enlargement from 1963 to 1992, and then stabilized until 2016.

The Matapédia river shows very little lateral migration that is furthermore very constant throughout all the period, with an average aggregated migration rate index (AMI) varying between 0.2 and 0.4 (Figure 9A). However, some specific subreaches are relatively high compared with the rest of the river, attaining an AMI of 1, mostly in the middle reaches. In contrast, the Petite-Cascapédia River depicts a much higher average AMI index throughout the years, varying from 0.7 to 2.0, with its highest during the period 1986–1992. During this period, reach 7 attained an AMI of 6.8%/yr, which is equivalent to a migration rate of 3.8 m/yr.

The analysis of the AMI at the reach scale helps define the general migration dynamics across homogeneous reaches (Figure 9B). Compared to the Petite-Cascapédia, reaches in the Matapédia are only marginally mobile, with an average AMI index varying between 0.1 and 0.6%/yr. Trajectories of change across reaches followed the same trends, where the peak migration was found in the period of 1985–1993, except for reach 2, where it was in 1963–1974 with a constant decrease in the following years. As for the Petite-Cascapédia, the highest migration rate was identified in the first reach during the period of 1963–1975 with a constant decrease in

**FIGURE 5** (A) Minimum, maximum and mean discharges of the maximum discharges during periods covered with aerial photographs, where blue bars show the number of ice jams that occurred during the specified period. (B) Spatiotemporal description of the number of jams throughout the river reaches and periods.



the following periods. Reach 1 and 3 followed the same kind of trajectories but reach 2 was at its highest in the period of 1986–1992. Across every reach, the lowest migration rate occurred during 1963–1974.

In the Matapédia River, the average rate of eroded or newly formed areas (m<sup>2</sup>/yr) was balanced, suggesting sediment equilibrium (Figure 10A). Slightly higher deposition occurred during 1963–1985 and 1993–2004. The period 1985–1993 saw more erosion than deposition but also the highest deposition rate (2.6%/yr), representing

nearly 2 ha of sediment. In the Petite-Cascapédia River, the differences between erosion and deposition were more pronounced. Periods 1963–1975 and 1986–1992 were dominated by deposition, with the highest rate (2.1%/yr) in the latter. These periods were interspersed with a strong erosion period (1975–1986) averaging 1.7%/yr erosion compared to 1.1%/yr deposition, mainly due to downstream avulsion and upstream enlargement.

The differences in the reach-averaged deposition and erosion rates highlight significant events (Figure 10B). In the Matapédia River,

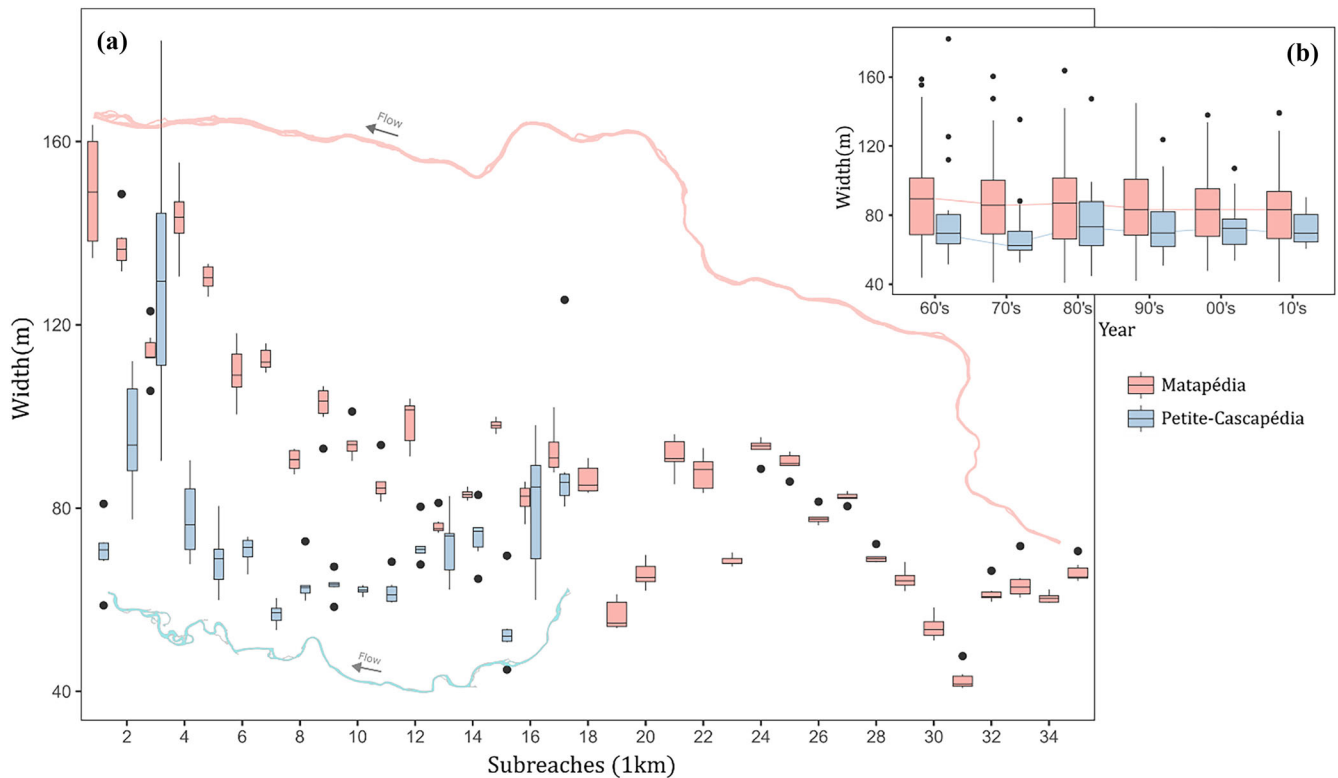


**FIGURE 6** (A) Width variation across subreaches. (B) Width variation across years. Fill colours distinguish Matapédia (red) from Petite-Cascapédia (blue).

the most significant erosion and deposition rates occurred in reach 1, where the deposition rate was dominant and increased until 2004, before abruptly changing to an erosion-dominated process between 2004 and 2016. In the Petite-Cascapédia, reach 1 shows strong variation with peaks in 1963–1975 and 1986–1992, and a low in 1975–1986. Reaches 2 and 3, although dynamic, show balanced trends with differences varying between  $-0.5$  and  $0.5\%/yr$ .

### 3.3 | Vegetation trajectory of change

The qualitative interpretation of land cover change shows that most of the changes occurred within the active channels (Figure 11). The main difference in terms of vegetation distribution across both rivers is the proportion of floodplains within the valley bottom, whereas the Petite-Cascapédia River has a much larger floodplain area, and thus an important forest proportion (Figure 10). Over the 60 years covered in this study, the overall trajectory of changes tended to increase vegetation cover and channel stabilization over both rivers.

The proportion of the different land covers across the active floodplain clearly shows important differences between the Matapédia and the Petite-Cascapédia, where water cover is largely dominant in the former and forest is most abundant in the latter, mostly because of the vast floodplains of the Petite-Cascapédia River (Figure 12A). In both rivers, a general decrease in anthropic area was combined with a significant increase in forest cover, mainly due to the abandonment of agricultural lands. Matapédia's forest cover ranged from 87 to 117 ha, while the forest cover of the Petite-Cascapédia River ranged from 371 to 443 ha (Table S4). These were the most noticeable general changes observed. The bare surface, sparse

vegetation and dense vegetation classes varied throughout the years, depicting a dynamic of progression and regression.

The rate of gain and loss of cover varied significantly throughout the different periods for both rivers (Figure 12B). In the Matapédia River, important gains in forest and dense vegetation were observed during 1963–1974, which can be explained by the abandonment of agricultural lands that underwent colonization by natural plant communities. In the other periods, the gains and losses of all land-cover classes were strongly variable. However, one interesting fact is the important increase in dense vegetation combined with a significant loss in bare surfaces and sparse vegetation in 1993–2004, suggesting the development of stable vegetated landforms through progression dynamics. Furthermore, this period was followed by a significant decrease in dense vegetation and an important increase in bare surfaces, depicting a period (2004–2016) of possible regression in many areas. In the Petite-Cascapédia River, important gains in forest cover were observed from 1963 to 2004. The period of 1986–1992 was the most active in terms of gain/loss, with large areas of bare and dense vegetated surface losses and significant gain in forest, suggesting a reconfiguration of the landscape mosaic. Other periods depicted sensitively similar changes according to the proportion of gain and loss of the different cover types. However, the period of 2004–2016 stands out with a significant gain in the bare surface.

The pathway of succession progression and regression for each type of vegetation class highlights the important differences between the two corridors (Figure 13). Noticeable differences were observed within the bare surface and the dense vegetation trajectory of succession. Regression areas of the bare surface (BS to WA) were much higher in the Matapédia River than in the Petite-Cascapédia River, with the  $l_{BS}$  being negative or neutral. In the Petite-Cascapédia

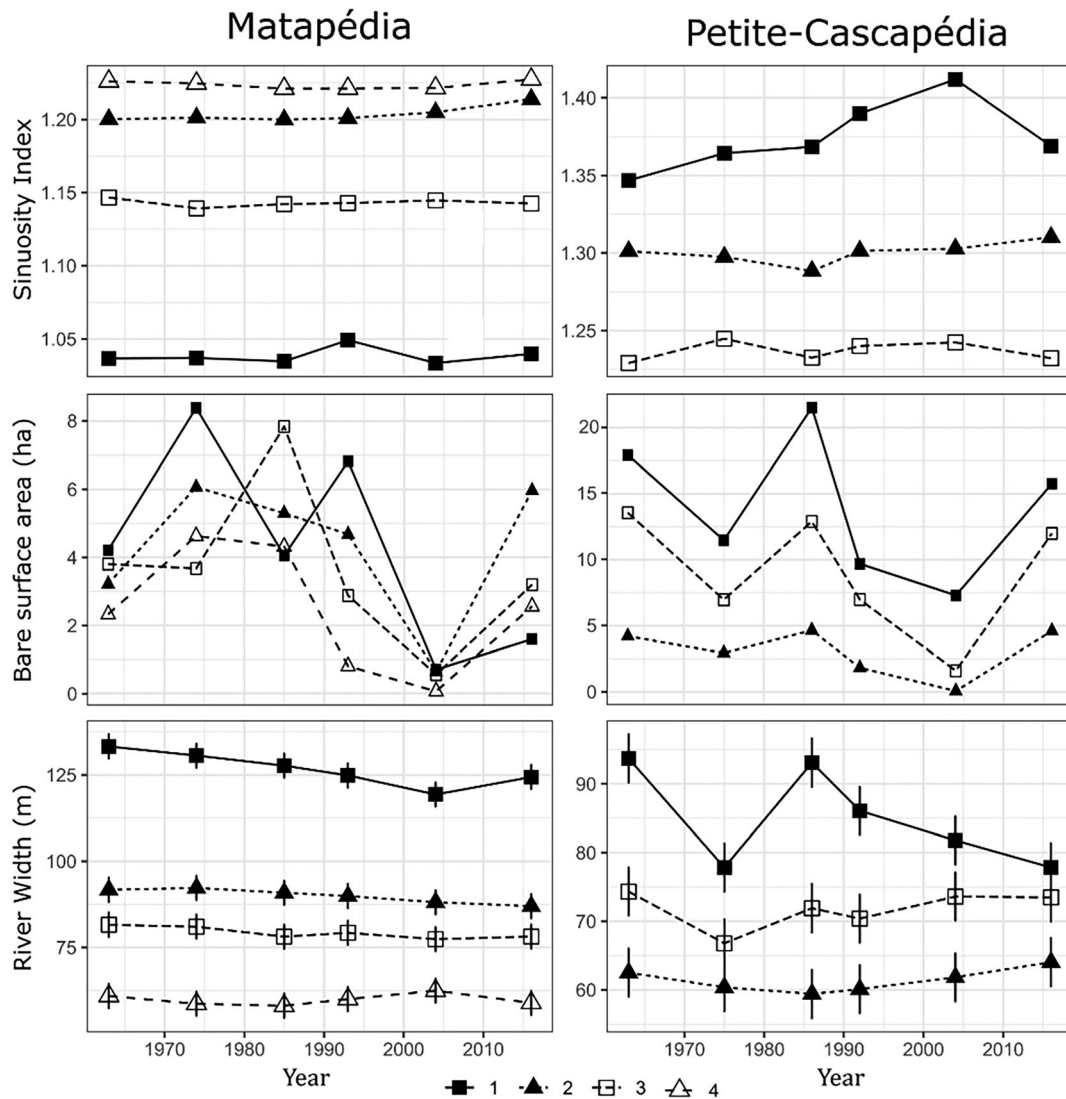


**FIGURE 7** Variation in sinuosity index, bare surface area and river width over time and selected reaches. Types of points and lines represent reaches from 1 to 4 for the Matapédia and 1 to 3 for the Petite-Cascapédia.

River, most of the bar surface areas progressed to a later successional state or stayed as is, where progression sometimes reached 40% of the total change, as in the period 1963–1975. Sparse vegetation progressed dominantly throughout all periods, with an important peak between the 90's and the 00's. This result shows the important development of dense vegetation patches throughout pioneer landforms and floodplains of both rivers during the entire study period. The main difference between the two rivers relies on dense vegetation dynamics, where the Matapédia River is mainly characterized by stability and the Petite-Cascapédia River by progression.

At the reach scale, the general succession pathways (every class combined) show a clear progression-dominant process in most of the reaches and periods (Figure 14). While the Petite-Cacapédia shows a balance of progression-dominant processes in all periods and all reaches (except for the period 1985–1993), the Matapédia show an alternating process of dominance between the periods. The periods of highest progression were 1963–1974 and 1985–1993 where a significant difference between progression and regression was shown, particularly for reaches 1 and 2. The periods 1974–1985 and 1993–2004 had more marginal areas of balanced succession, and some even tended to be a regression-dominant process. In the Petite-Cascapédia River,

almost every reach during every period shows a progression-dominant dynamic, where Reach 1 (1986–1992) stands out according to the rate of changes. The only regression-dominated dynamics happened in Reach 1 during the period of 1975–1986 and in Reach 2 during the period of 2004–2016. Yet, the intensity of those regression dynamics remains very low when compared to the other rates of change.

The overall index of succession ( $I_{all}$ ) was calculated for every sub-reach to analyse the trajectories across spatial and temporal scales (Figure 15A). This representation helps to identify specific areas of progression- or regression-dominant processes, and the magnitude of these changes compared to the total area of change. When averaged across the entire rivers, indexes balance out and depict a very small proportion of change, except for some exceptions such as the period 1963–1974 in the Matapédia River with an index of 0.2. However, the peaks of progression and succession can easily be identified through different subreaches and periods. Overall, the Matapédia River shows much higher variation along its rivercourse than the Petite-Cascapédia River. The period 1963–1974 significantly stands out compared to the other periods, with an average  $I_{all}$  stating that 20% of all changes were progression changes. On the other side, the period 1974–1985 shows the only negative  $I_{all}$ .

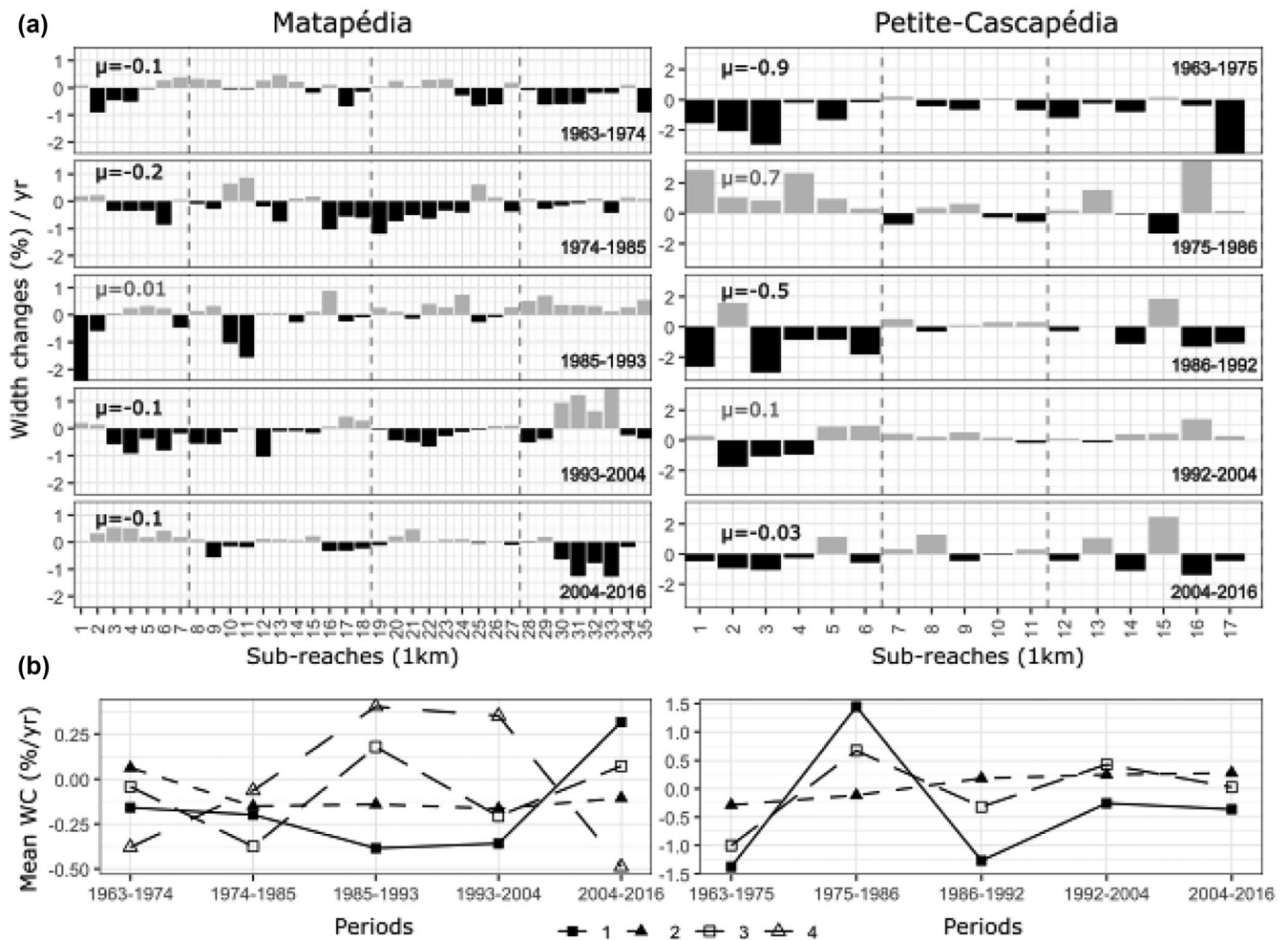


**FIGURE 8** (A) Variation in width across periods and subreaches for both rivers. The colours of the bar distinguish narrowing (black) from widening (grey) processes. The increase/decrease in width was standardized by the mean width of each subreach and divided by the number of years in a given period. Vertical dotted lines mark the limits of each selected reach. (B) Mean changes in the standardized width change rate across the selected reaches. The line and point types distinguish the reaches.

Upscaling to the reach scale helps to identify trends of  $I_{all}$  (Figure 15B). In the Matapédia River, reaches 1 and 2 are closely correlated according to their trajectories, with alternating periods of progression-dominance and regression-dominance. Reach 3 only varies between 0.08 and 0.11, showing very little dominant process. Regression peaks were found in reaches 2 and 4, at the period-1974-1985 and 1985-1993, respectively. In the Petite-Caspédia River, reach 2 and 3 follow the same trajectory, but reach 1 stands out with two peaks of progression-dominance reaching an  $I_{all}$  of 0.15 accounting for 15% of total change equivalent to progression. The average reach index was positive along every reach of the PC, suggesting that progression is constantly the dominant area-related process.

## 4 | DISCUSSION

The results exposed important variations according to the vegetation and channel planform trajectories, both at the inter-river and inter-reach scales. A synthesis of the results is presented in Figure 16 to agglomerate the principal channel adjustments and vegetation progression/regression dynamics. The following

section examines the role of ice jam dynamics on trajectories and discusses river-vegetation interactions from a biogeomorphological perspective.

### 4.1 | Role of ice-jams and floods on channel planform and vegetation trajectories

Previous studies have explored the impact of ice jams on river channel dynamics such as channel enlargement, riverbed erosion patterns, riverbank morphology and avulsion dynamics (Beltaos, 2016; Kolarski & Shen, 2015; Morin et al., 2015; Smith & Pearce, 2002). One specific study by Boucher et al. (2012) associated channel enlargement with recurrent ice jams, in which enlargement of up to 1.5 to 2 times the initial channel width was observed in reaches subjected to strong jamming, such as in the presence of meander or islands. These processes are caused by (1) the pressure exerted on the banks during the accumulation of ice blocks and (2) the release of jams that exert strong shear stress and remobilize the sediment (Boucher, 2017; Boucher et al., 2009). Although not true over each reach in our study, some observations corroborate this claim. For example, one of the largest enlargements in the Matapédia River

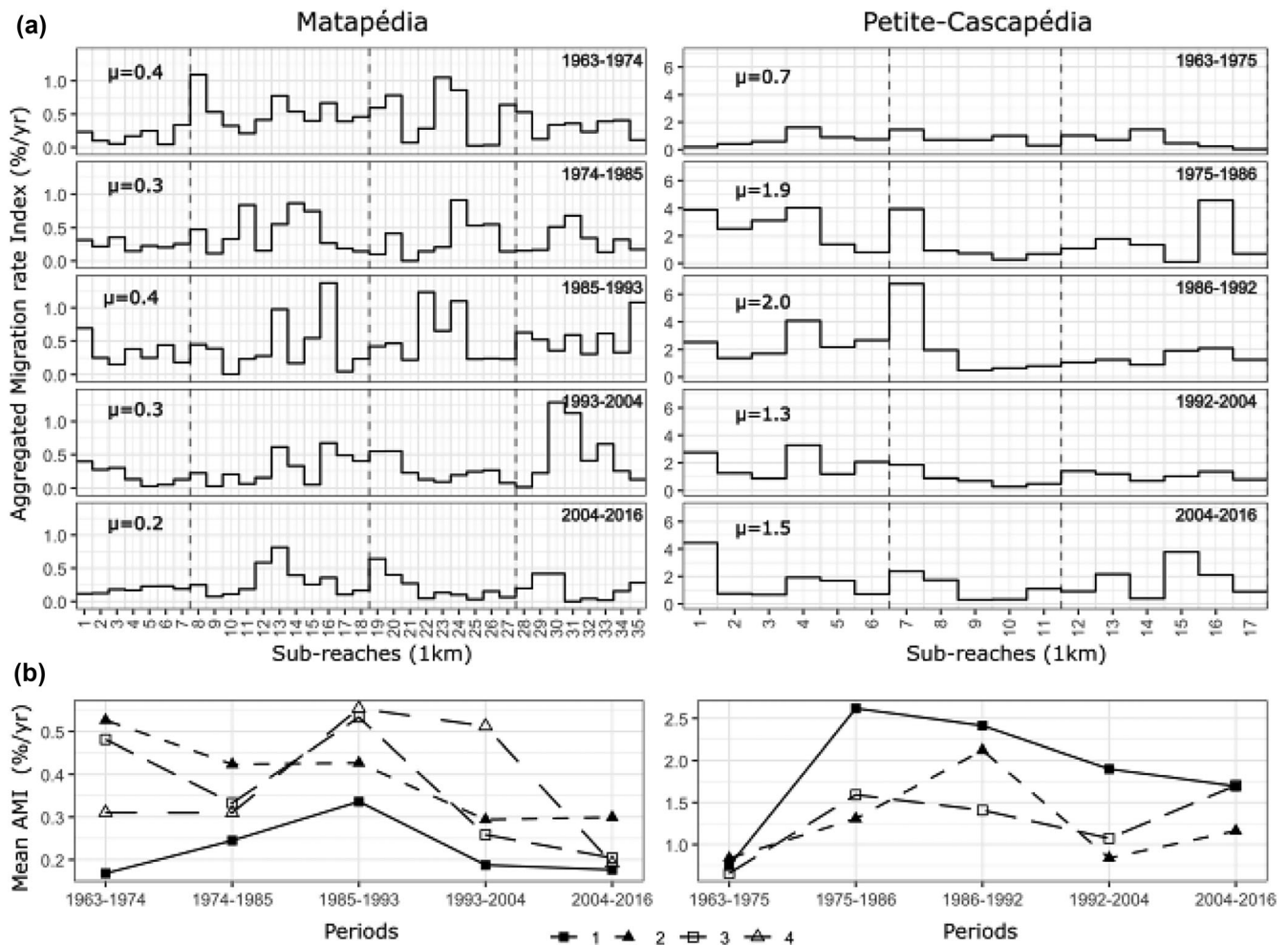


**FIGURE 9** (A) Aggregated migration rate index (AMI) across periods and subreaches for both rivers. The AMI value was standardized using the mean width of each subreach. Vertical dotted lines mark the limits of each selected reach. (B) Mean changes in AMI across the selected reaches. The line and point types distinguish the reaches.

occurred in reach 1 during the period of 2004–2016 when multiple ice jams occurred. However, enlargement also occurred in the fourth reach during the period of 1985–1993, which presented no sign of a confirmed ice-jam (Figure 16). These effects can be localized and affect a very restrained portion of a river because of channel morphological features (e.g., steep narrowing, meander and slope change), fostering the formation of localized ice jams (De Munck et al., 2017). Figure 6 shows a high variability in channel width changes, with localized enlargements and narrowing throughout the subreach scale. Such results suggest that some of the localized important enlargement (e.g., subreaches 10 and 11 during the period 1974–1985) could be caused by local ice jam processes. However, such variability also appears in periods without ice jams, indicating that ice jams are not the ultimate enlargement factor in such rivers that are also responsive to flood events.

In a modelling study, Kolerski & Shen (2015) found that during a moderate magnitude ice jam in 1984 on the St. Clair river (Michigan, USA), bed shear stress during the ice jam was not significantly higher than during free-flowing water floods, which was attributed to important water depth with thin ice jam. Aligned with the latest, both the Matapédia and Petite-Cascapédia rivers had the highest erosion rates during periods with low to no ice jam activity (Figure 16). This suggests that ice jams are not the principal factor

contributing to channel erosion and sediment mobilization at the corridor scale. The highest erosion rates in the Matapédia River were observed between 1974 and 1993 when the highest floods were recorded ( $Q_{50}$  and  $Q_{20}$ ). However, on the Petite-Cascapédia, the highest erosion rate was observed during the period (1986–1992) with floods as low as  $Q_5$  and no ice jams events. This observation could be explained by the fact that the Petite-Cascapédia River is subjected to many avulsions and that this period could be dominated by strong bar push dynamics, increasing lateral migration. Furthermore, this supports the idea that ice dynamics might not be a critical factor in channel dynamics compared to sediment dynamics and flood regimes.

Ice jams can exert significant physical disturbances on vegetation stands by wounding, shearing, toppling and even uprooting ligneous species located on bars, riverbanks and floodplains, thus creating new colonizable open sites from vegetation to establish (Lind et al., 2014; Rood et al., 2007; Vandermause et al., 2021). In a study on the Peace River (Canada), Uunila & Church (2014) have observed recurrent patterns linking the frequency and magnitude of ice jams with the composition and age structure of riparian plant communities, suggesting that succession dynamics were significantly influenced by ice jams, especially in the lower riparian communities closest to the river. These turnover events were also observed by

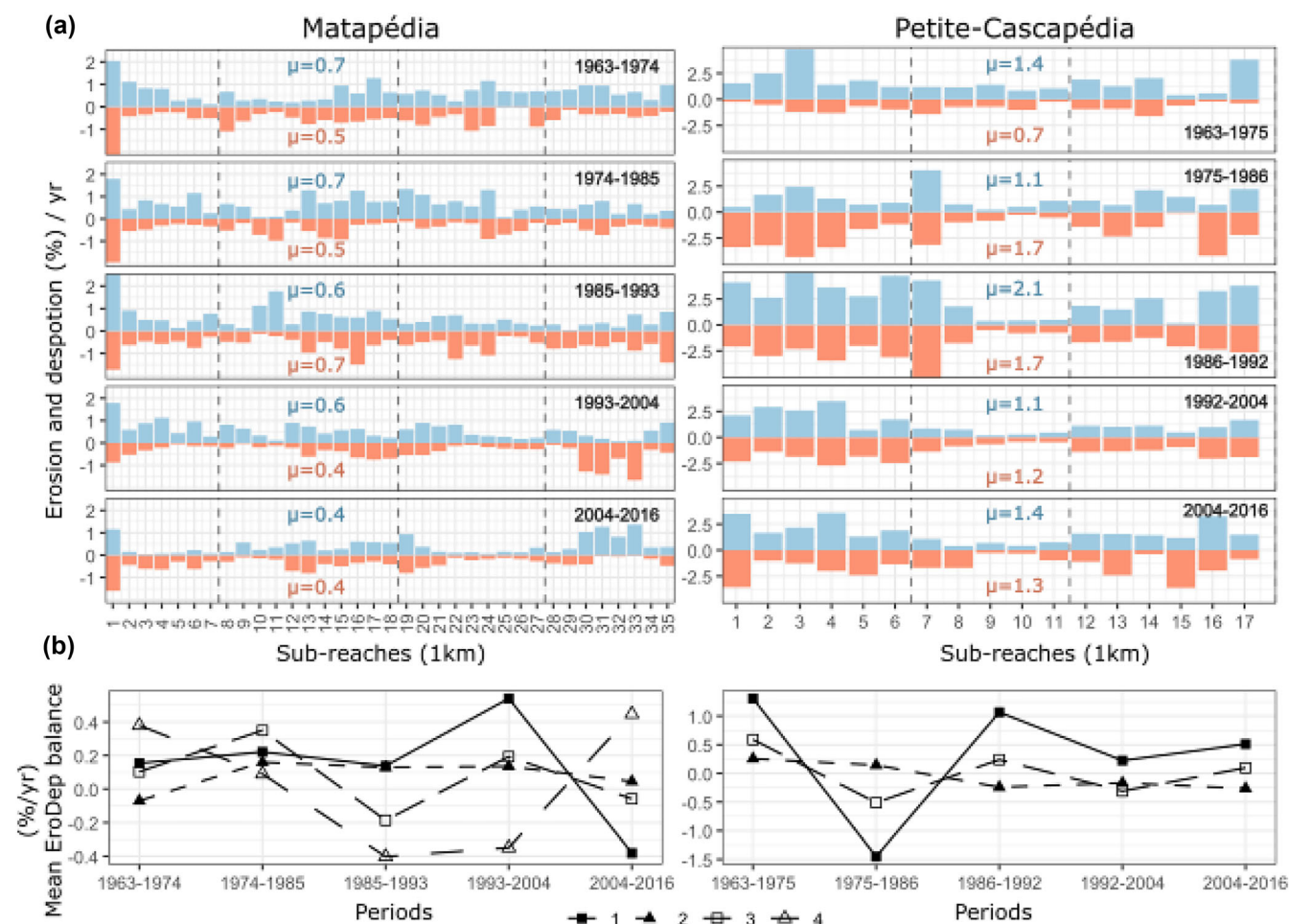


**FIGURE 10** (A) Erosion and deposition rates across periods and subreaches for both rivers. The colours of the bar distinguish erosion (orange) from deposition (blue) processes. The erosion-deposition areas were standardized by the mean area of each subreach and divided by the number of years in each period. Vertical dotted lines mark the limits of each selected reach. (B) Mean balance of erosion-deposition rate (difference between deposition and erosion) across selected reaches. The line and point types distinguish the reaches.

Rood et al. (2007) and Smith & Pearce (2000) on the Milk River (Alberta and Montana) and the Oldman River (Alberta), respectively. They both found areas where ice jams generated open sites with ideal conditions for the emergence and establishment of pioneer ligneous species such as cottonwood and willow species. Matapédia's results effectively capture these dynamics where high regression happens during years of frequent ice jams. For every period where an ice jam happened 1 or 2 years prior to the latest photograph, the affected reach and subreaches within it depicted a dominant regression trajectory, suggesting a significant effect on the vegetation turnovers (Figure 16). These results align with previous studies stating that ice jams are the leading factor of vegetation rejuvenation within these systems. Furthermore, high regression rates were also observed in periods with low-magnitude floods but in the presence of ice jams. For example, reach 2 in the period of 1993–2004 shows high regression that can only be explained by the presence of multiple ice jams, as the only floods that occurred during this period were the equivalent of 2-year recurrence floods. This implies that ice dynamics can exacerbate the effect on vegetation rejuvenation during moderate floods that would probably cause no vegetation removal without ice. While similar patterns are observed on the Petite-Cascapédia, they are less pronounced, suggesting that confined rivers' vegetation communities are more prone to repetitive

rejuvenation. Confined rivers are known to affect flow structure by increasing their water depth compared to a mobile river with the same discharge, thus increasing the shear stress and applying considerable drag forces onto riparian vegetation (Dufour et al., 2007). Ice impacts might behave alike and be more impactful in confined rivers compared to mobile rivers.

While uncertainties remain along the impact of flood against ice onto the channel trajectories and vegetation succession, our results suggest that ice dynamics controls first and foremost vegetation rejuvenation. Other studies have quantified the important impact on sediment transport, erosion and deposition resulting from ice jam dynamics (Beltaos, 2016; Ettema & Kempema, 2012; Turcotte et al., 2011; Vandermause et al., 2021), but the two-dimensional planimetric assessment of erosion and deposition presented in this study could not confirm a relationship between ice jams and erosion. This could be explained by two main reasons. First, it could be caused by the precision of the data where gaps of 10 years between photographs may not be sufficient to evaluate with precision the eroded area specifically provoked by mechanical ice erosion such as the year-scale assessment of erosion studied by Vandermause et al. (2021). This suggests that ice-dynamics may play an important role at the local and monthly/annual scale but that their effects are mitigated at the corridor and multidecadal scales.

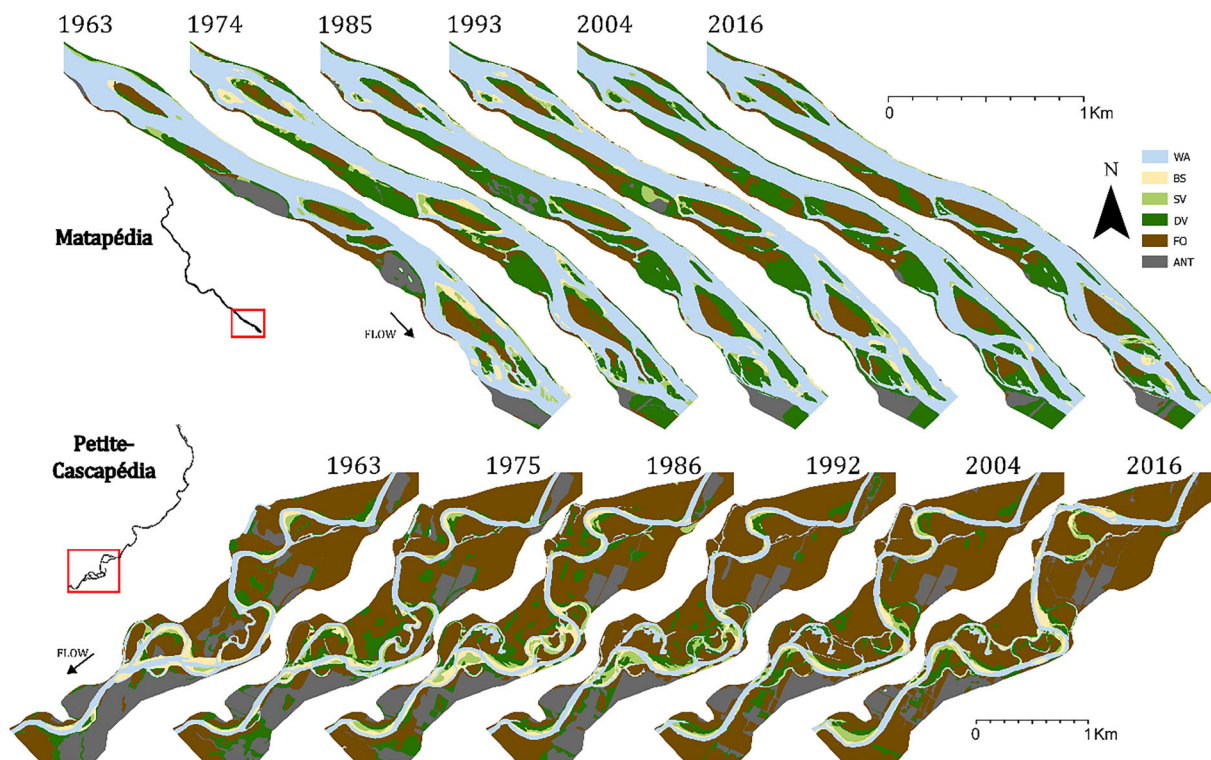


**FIGURE 11** Classification map resulting from the photo-interpretation of the different land covers (WA: water, BS: bare surface, SV: sparse vegetation, DV: dense vegetation, FO: Forest, ANT: anthropic). These are samples of the most downstream and dynamic reaches of both rivers.

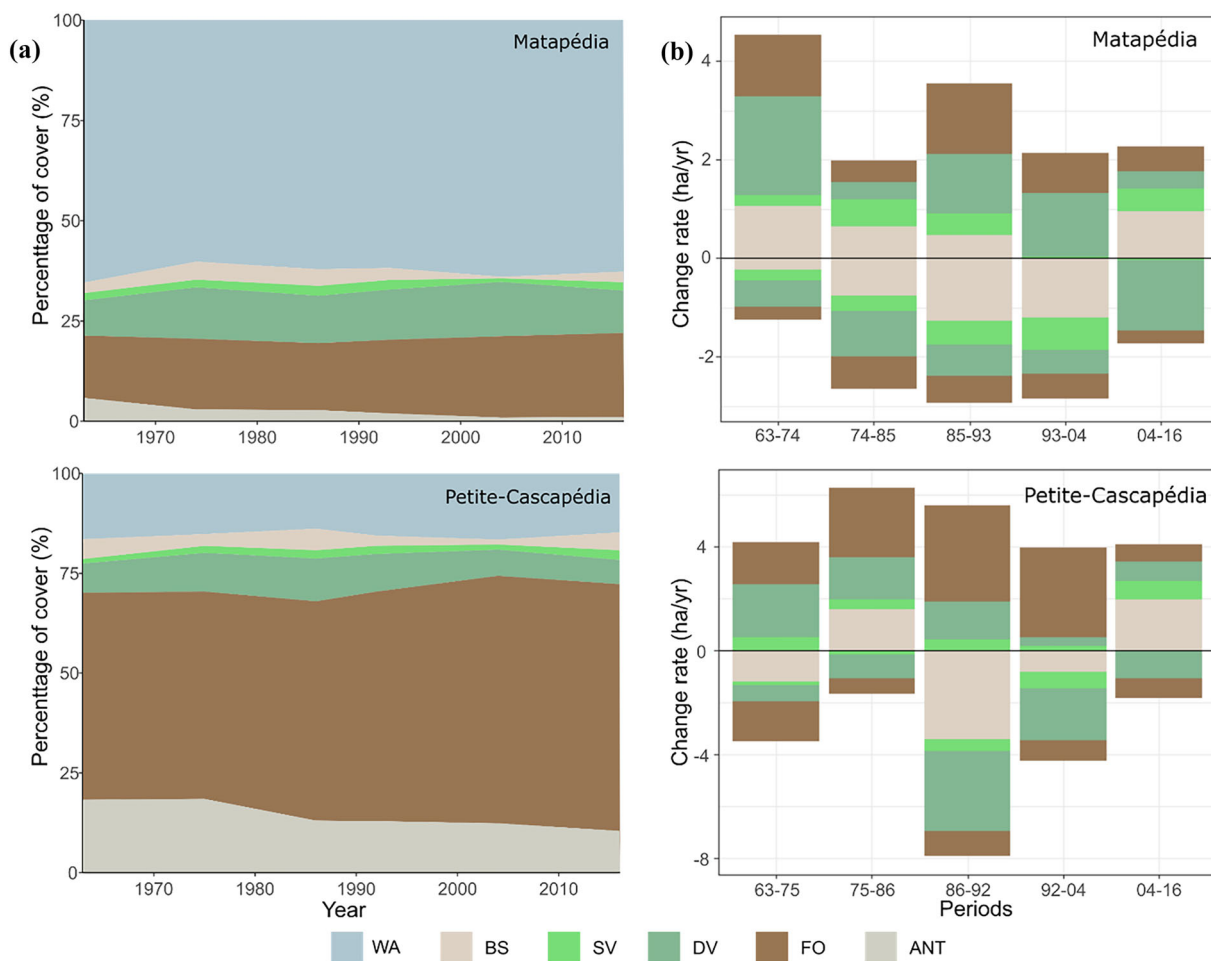


**FIGURE 12** (A) Proportions of surface cover classes for each year. (B) Change rate of cover classes over time showing gain and loss between periods. Negative values represent loss surfaces and positive values represent gained surfaces between two years.

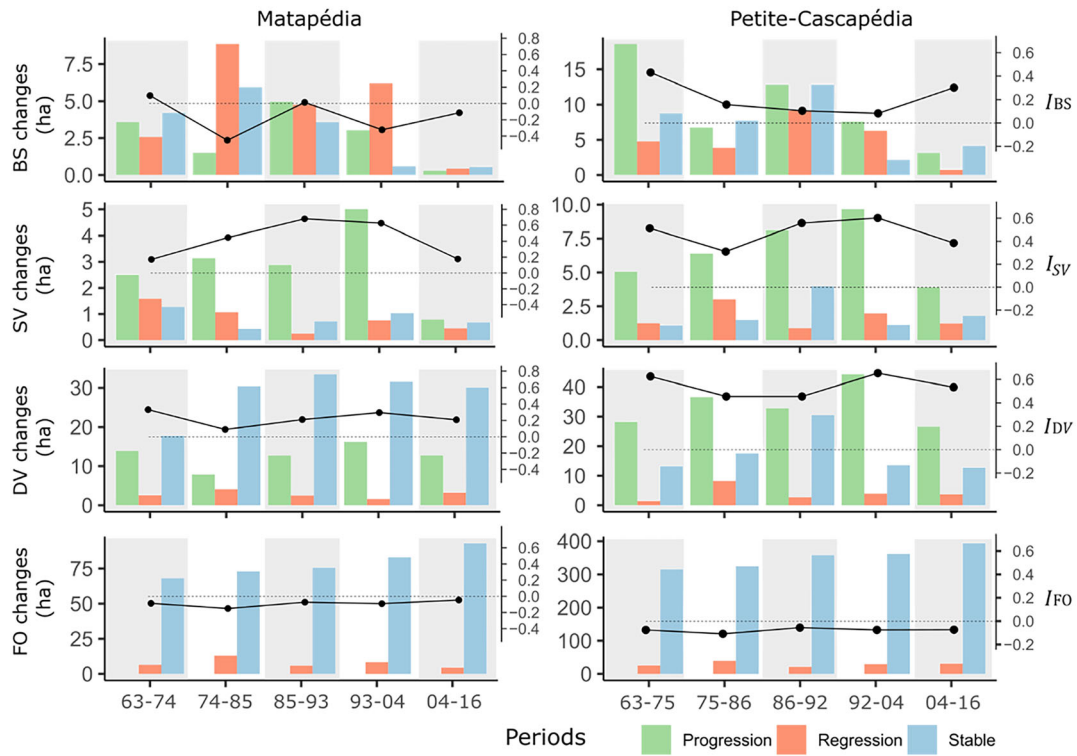


**FIGURE 13** Trajectory of succession processes for each class of surface cover during different periods. The coloured bars represent the area of progression (green), regression (red) and stability (blue). The progression area represents a change from the initial cover to a later successional state, regressing the area that passed from the initial cover to an earlier successional state and the stability of the area that depicted no change. The line graph on the secondary axis shows the trajectory of the indexes measuring the dominant process and its importance compared to the total area of change.

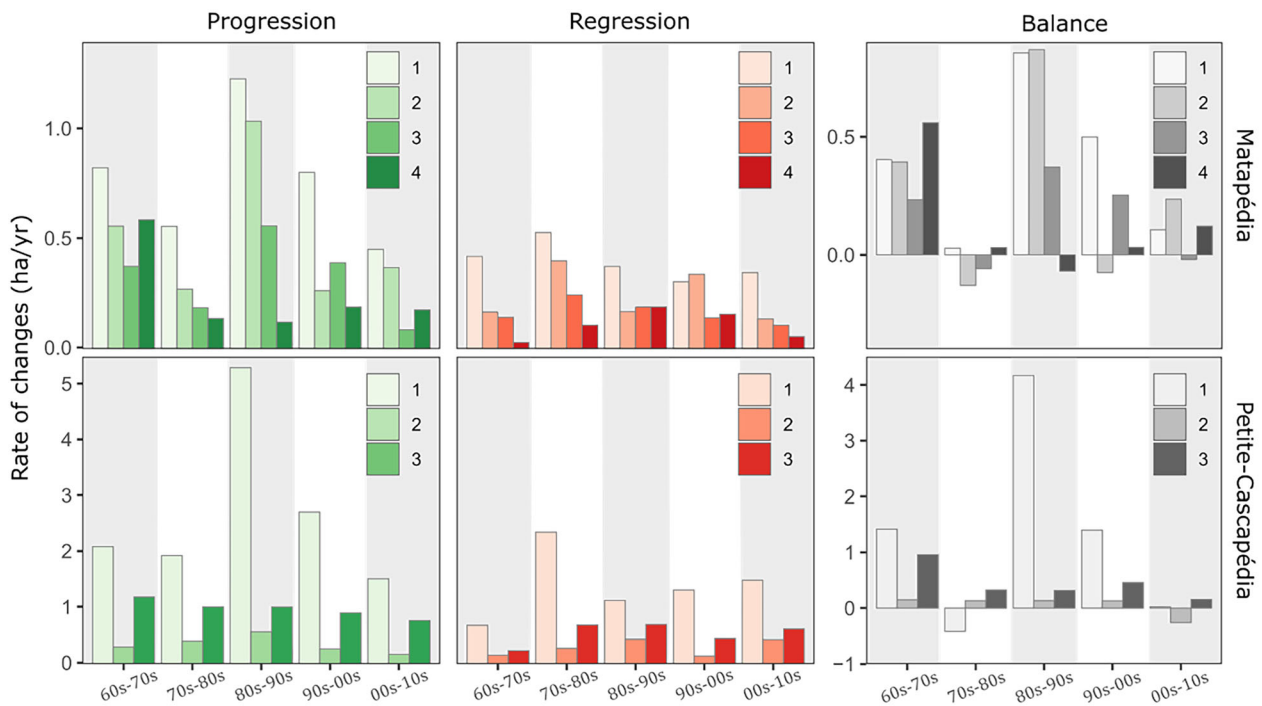


**FIGURE 14** Rate of change in succession path through specific reaches and periods. Progression changes depict all progression pathways, similar to regression. Balance is the difference between the progression and regression rates. The colours of the bars represent the path of succession (green for progression; red for regression; grey for balance), and the colour gradient represents the reach number (1 to 4: light to dark).

Second, it could be explained by the important water depth increase during breakups, which increases the distance between the riverbed and the ice blocks. As such, ice-related erosion forces might

principally be applied on ligneous vegetation and not on the riverbed, causing vegetation scouring and uprooting without significant sediment erosion.

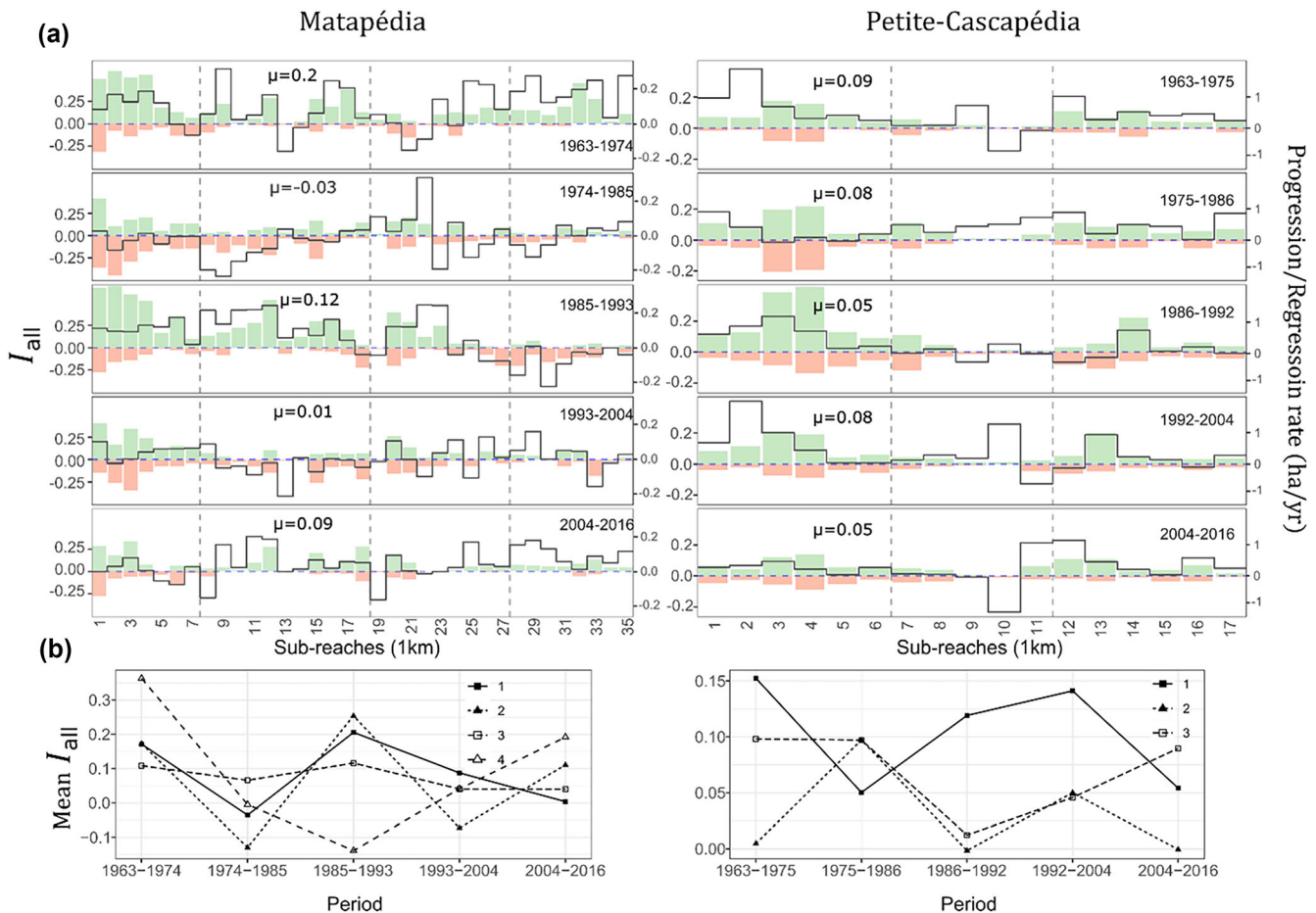


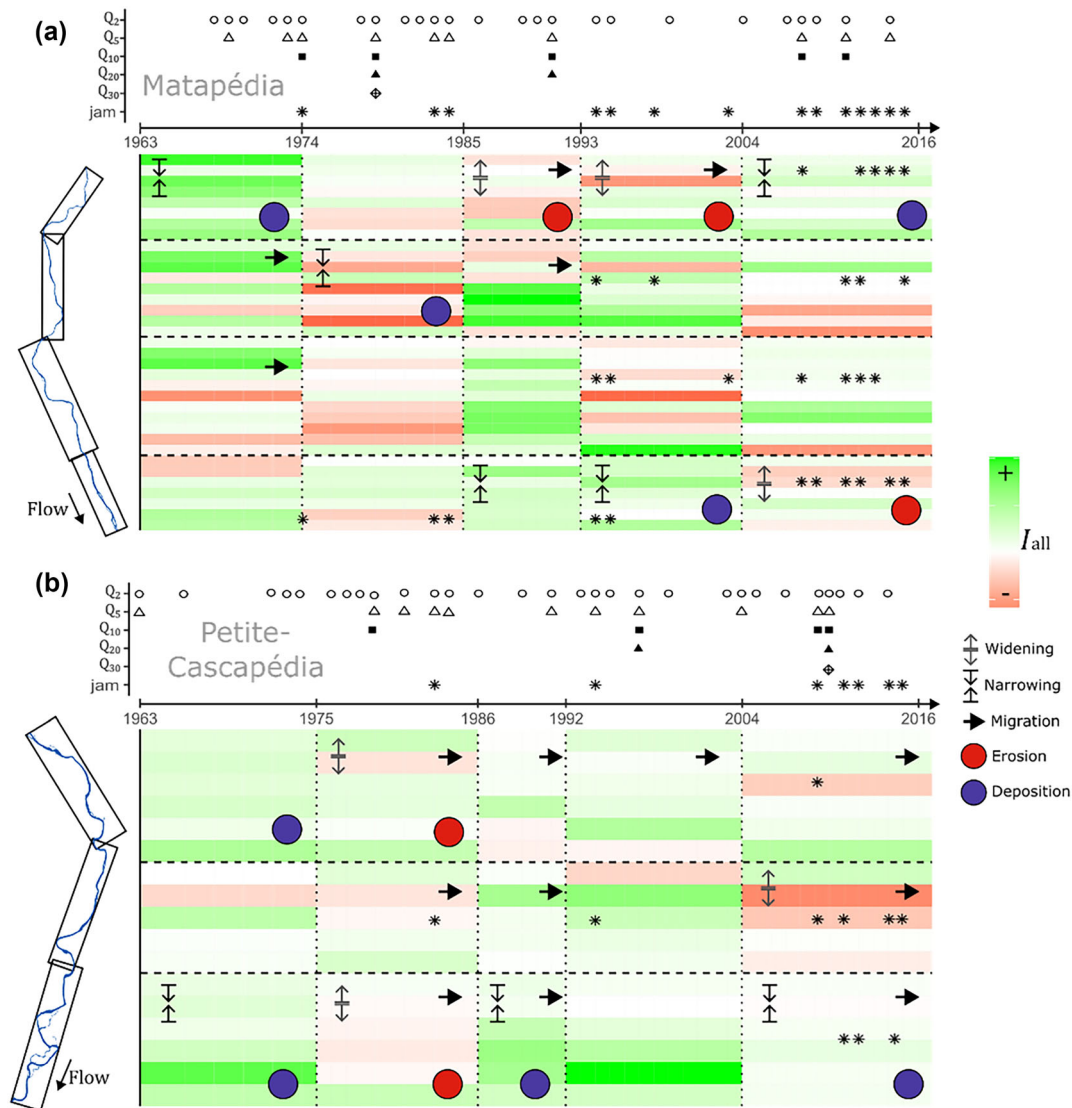
**FIGURE 15** (A) The  $I_{all}$  index value across periods and subreaches for both rivers (left y-axis), along with the progression (green) and regression (red) rates of each subreach (right y-axis).  $I_{all}$  is calculated with every succession path (see methods for details), where positive and negative values indicate a dominance process of progression and regression, respectively. The closer the value is to  $-1$  or  $1$ , the more important is the dominant process. (B) Mean  $I_{all}$  values across the selected reaches. Line and point types distinguish the reaches.

## 4.2 | Biogeomorphological behaviour interpretation

Fryirs (2017) defines river behaviour as the “adjustments to river morphology induced by a range of erosional and depositional mechanisms by which water moulds, reworks and reshapes fluvial landforms, producing characteristic assemblages of landforms at the reach scale”. For the following discussion, we will focus on the biogeomorphological dynamics that participate in these sets of processes shaping river channels and planforms. More specifically, it concerns the dynamic and reciprocal interactions between plants and geomorphological processes, in order to assess the bidirectional effects between geomorphology and vegetation, the co-adjustment between landforms and vegetation type and the emergence of biogeomorphological units fostered by these interactions (Bywater-Reyes et al., 2022; Corenblit et al., 2007; Corenblit, Piégay, Arrignon, González-Sargas, Bonis, Davies, et al., 2024; Corenblit, Piégay, Arrignon, González-Sargas, Bonis, Ebengo, et al., 2024; Gurnell & Bertoldi, 2024). However, it is worth noting that disentangling cause-and-effect within biogeomorphological system is more complex at the reach and fluvial corridor scales, i.e., to discern whether vegetation primarily responds or drives geomorphic processes or if co-adjustment processes are dominant (Corenblit, Piégay, Arrignon, González-Sargas, Bonis, Davies, et al., 2024). Our results cannot provide an absolute

and clear interpretation of the ongoing dominant process within both rivers because of (1) the lack of annual aerial data and sparse historical information related to ice activities, and (2) the fact that we did not monitor sediment volume and plant traits through consecutive years to find relationships. However, our results remain a first step in the exploration of these dynamics in those understudied hydrosystems and suggest different behaviours and reactions to disturbances that can let us pose hypotheses about the biogeomorphological dynamics driven by flood and ice disturbances.

Riparian vegetation is known to increase bank shear strength from root systems binding soil particles, decrease water shear stress by reducing flow velocities and promote sediment deposition by the reduced flow velocities (Andreoli et al., 2020; Bywater-Reyes et al., 2022; Corenblit et al., 2007). For instance, experimental studies from Tal & Paola (2010), Kyuka et al. (2021) and (Yang et al., 2018) all demonstrated that dense vegetation cover significantly reduced channel migration rates, fostered narrower and deeper channel, decreased erosion rate and slowed down widening processes. These observations were also made in real-world study cases, for example in the Sacramento River and the Tarim River (Micheli et al., 2004; Yu et al., 2020). Our results on the trajectories of channel changes and vegetation succession indicate potential biogeomorphological feedback within both systems. While it was not part of the principal results due to its lack of statistical significance and qualitative nature,



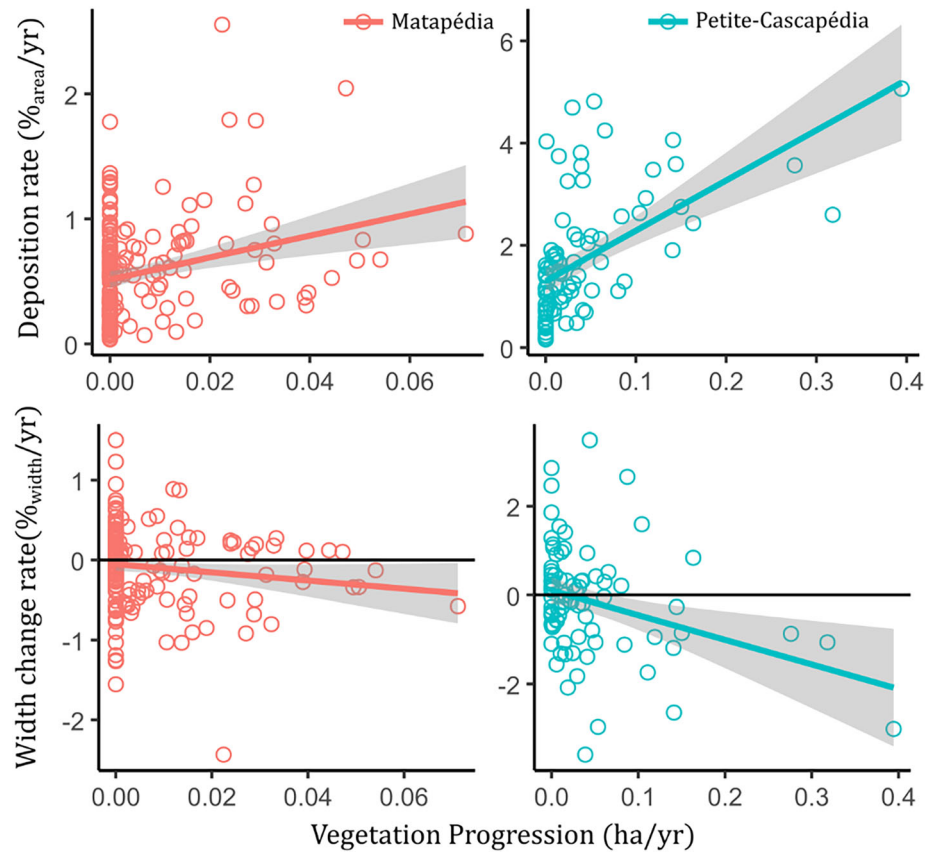
**FIGURE 16** Synthesis figure agglomerating both dominant vegetation progression/regression dynamics at the sub-reach scale and significant/dominant channel adjustment at the reach scale, along with a summary of the disturbances. The timeline on the top of the graphs identifies years when a certain disturbance occurred (empty circle for  $Q_2$ , empty triangle for  $Q_5$ , solid square for  $Q_{10}$ , solid triangle for  $Q_{20}$ , lozenge for  $Q_{50}$  and star for ice jams) at the corridor scale. Ice jam years (stars) were also reported spatially in the synthesis figure to spatialize known jams throughout the reaches. Circle and arrow symbols show the dominant hydrogeomorphic processes and are based on the average value. Migration (presence or absence of a lateral arrow) and widening/narrowing (diverging grey arrows for widening and converging black arrows for narrowing) are shown when the values are larger than the RMSE. Erosion (red circle) or deposition (blue circle) is shown when one of the processes is more important than the other in a given reach.

Figure 17 supports this idea by showing relationships between vegetation progression rates, width change rate and deposition rate. At the subreach scale, the higher the progression rate (i.e., development of dense vegetation cover), the higher the depositional rate and narrowing process. It remains hard to distinguish whether the channel changes have let vegetation progress, vegetation forced the channel to adjust, or if complex interactions led to these results. We can however hypothesize that potential feedback has occurred based on the previous studies that confirmed these dynamics and the observations made in this study. The synthesis also strongly supports these hypotheses, depicting a pattern where periods following important turnovers and erosion are characterized by channel narrowing and vegetation progression.

In the Matapédia river, the period of 1974–1985 depicted the highest progression rate (Figure 12) and was instantly followed by

channel narrowing processes ranging from 2 to 7 m, combined with the lowest erosion rate and the lowest lateral migration rate over the entire study period (Figures 8, 9 and 10). Islands constantly aggraded since 1963 and some pioneer landforms such as lateral and central bars emerged in 1985. As island formation is known to be strongly impacted by vegetation and its effects on water flow (Bertoldi & Gurnell, 2020; Gurnell & Bertoldi, 2020), we can hypothesize that vegetation communities in the Matapédia River act as a stabilizing factor. Furthermore, some of the emerging pioneer islands were maintained within the river for decades even after years of important ice jam activities, suggesting induced resistance from vegetation root systems stabilizing these pioneer landforms. Same patterns were also observed in the Petite-Cascapédia, where a high progression rate from the period of 1986–1992 was followed by a relatively low migration rate, little changes in river width and a positive ratio of

**FIGURE 17** Relationship between sparse/dense vegetation progression rate and deposition/width change rate. Horizontal lines in the width change plots delimit narrowing (negative) and widening (positive). Each point (red for Matapédia; blue for Petite-Cascapédia) corresponds to a specific subreach in a specific period. The deposition rate was normalized based on the average channel area of each sub-reach. The width change rate was normalized based on the average channel width of each sub-reach. Regression line is based on the ordinary least squares.



deposition/erosion rate (Figures 8, 9 and 10). These observations suggest the extension of bar surfaces and the emergence of new floodplain areas (in the case of channel migration), followed by vegetation encroachment and sediment stabilization leading to a narrowing process of the channel.

Resilience in the biophysical realm of rivers can be defined as the ability of a river system to return to its original state after a disturbance (Corenblit, Steiger, Dufour, et al., 2024). The rate at which landforms and vegetation recover after a disturbance are great indicator of the potential resilience capacity of a system. Our study suggests high resilience potential in both rivers despite frequent mechanical ice breakups, which vary according to their unique behavioural regime. Based on the Green Balance Model (Bywater-Reyes et al., 2022), the two studied rivers are great examples of rivers where vegetation acts as a geomorphic agent by narrowing the channel through sediment stabilization and accumulation. As depicted in Figure 15A, the rivers exhibited a dominant progression process in terms of vegetation succession after each regression phase, indicating the potential of these systems to rapidly recover from disturbances. Despite localized vegetation turnovers and channel impacts (erosion/enlargement) that followed ice jams periods, a relaxation time of less than 10 years was sufficient for vegetation encroachment and landform stabilization. Figure 17 clearly shows this process. Despite years with some significant changes in channel structure and vegetation distribution, the rivers re-adjusted quickly to the same fluvial style it was beforehand. Ice disturbances thus might play a role in the turnover rates and as factors of channel changes but clearly do not act as important inhibiting factors to the biogeomorphological dynamic equilibrium at play. These observations supports findings done in a Mediterranean river where general trends of vegetation progression were punctuated with

irregular rejuvenation followed by high resiliency of the biogeomorphological structure (Corenblit et al., 2010). The only difference between these observations is the source of disturbance, where rejuvenation rates were controlled by intense irregular floods in the Mediterranean context and by intense irregular ice jams events in our study.

Riparian species such as willows (*Salix* sp.) and poplars (*Populus* sp.) have evolved and adapted to regular and chaotic hydrogeomorphological regimes by developing specific morphological and biomechanical traits allowing them to successfully establish, grow and disperse in these highly dynamic environments (Bornette et al., 2008; Edwards et al., 1999; Karrenberg et al., 2002; Lytle & Poff, 2004). Even though our results indicate high resilience of vegetation communities following ice disturbances, they also denote a lack of resistance by notwithstanding periods of ice jamming events. This observation suggests that the isolated and sporadic regime of ice jams is not sufficiently regular for riparian species to develop long-term resistant adaptations to these specific disturbances. Thanks to their flood-related adaptations giving them the ability to resprout quickly, they can still maintain their presence in such environment through resiliency by avoiding high mechanical stresses.

## 5 | CONCLUSION

This study examined the long-term effects of ice dynamics on channel planform adjustments and vegetation trajectories within two contrasting cold rivers: the confined Matapédia River and the mobile Petite-Cascapédia River in the Gaspé Peninsula of Quebec, Canada. The study used dendrochronological analysis, historical data and a diachronic

analysis of aerial photographs from 1963 to 2016 to evaluate the influence of ice dynamics on river evolution. Even though precise discernment between the impacts of flood versus ice was not noticeable, the results suggest many interesting points related to the long-term effects of ice jams on cold rivers biogeomorphological dynamics.

First, while previous studies have shown that ice jams could cause important channel erosion, no clear effects were observed at the multidecadal scale when compared with the flood regime. This suggests that relaxation time between ice jam disturbances was sufficient to recover channel forms and plant communities. Second, ice jams first and foremost affect vegetation by causing turnovers. These rejuvenations could however have indirect effects on channel erosion due to the removal of vegetation-induced shear strength applied to banks. Third, the presence of ice jams can exacerbate the potential of vegetation turnovers during periods of low-discharge floods. Results have shown that high regression occurred during very low flood periods with the presence of ice jams, suggesting the role of ice in increasing shear strength. Fourth, the construction of pioneer biogeomorphological units seems to be active despite the presence of ice dynamics, as shown by the relations between sediment deposition and the rate of vegetation successional progression. Fifth, while being two contrasted behavioural systems with different responses to disturbances, both rivers exhibited biogeomorphological resilience. The Matapédia's resilience is shown by its quick rejuvenation of vegetation communities that underwent turnovers. The Petite-Cascapédia, on its hand, was quickly adjusting to channel changes (e.g., migration and avulsion) and establishment of new communities.

These results are a first step towards the exploration of the interactions between ice disturbances, channel adjustment and vegetation succession. However, further research is needed to better quantify and assess the extent to which the ice jam regime affects the turnover rate and the biogeomorphological construction of landforms. We propose that long-term monitoring of vegetation and geomorphological adjustments at the local and reach scales must be established to accurately understand the interactions between ice dynamics, vegetation and hydrogeomorphological dynamics.

Finally, this study focused on ice jams at the fluvial corridor scale with ice scars used for ice dynamic characterization. However, these proxies only reflect high-magnitude events and do not consider mechanical breakups restrained below the floodplain level. Even if no ice jams or high magnitude breakup happens, we believe that the shear force associated with moderate ice breakups might play a role in vegetation development and succession. Exploring the response and effect functional traits of these communities would serve greatly to find relationships between plant communities' structure/composition and northern river ice dynamics. Future research must focus on these processes that might be much more frequent but less destructive than large ice jam breakups. These approaches are especially essential in a climate change context where mechanical ice breakups and ice jams might become more frequent due to more frequent winter thaws. Thus, tackling down the role of these disturbances in the moderate- to long-term evolution of rivers is essential for efficient management.

#### AUTHOR CONTRIBUTIONS

Mathieu Prugne: Conceptualization, methodology, investigation, writing—initial draft, writing—reviewing and editing. Dov Corenblit:

supervision, methodology, writing—reviewing and editing. Maxime Boivin: supervision, methodology, writing—reviewing. Thomas Buffin-Bélanger: funding acquisition, supervision, methodology, writing—reviewing and editing.

#### ACKNOWLEDGEMENTS

This research was financially supported by the Natural Sciences and Engineering Research Council of Canada (grand ID: RGPIN-2023-05431; grant owner: Thomas Buffin-Bélanger). Special thanks to all research professionals and assistants from the *Laboratoire de recherche en dynamique et géomorphologie fluviale* (LGDF) who helped gathering data during field work and helped with tree samples preparation. We also want to thank Dominic Arsenault from the UQAR for giving the access to his dendrochronological lab. Finally, we thank the reviewers who took the time to review this paper and provide constructive feedback to enhance the quality of writing and precision of content in the manuscript.

#### CONFLICT OF INTEREST STATEMENT

The authors declare that they have no conflicts of interest relevant to this study.

#### DATA AVAILABILITY STATEMENT

Datasets that have been used and analysed in this study can be shared on demand by contacting the corresponding author.

#### ORCID

Mathieu Prugne  <https://orcid.org/0000-0002-2452-973X>

Dov Corenblit  <https://orcid.org/0000-0002-2431-7913>

Maxime Boivin  <https://orcid.org/0000-0002-1248-8061>

#### REFERENCES

- Andreoli, A., Chiaradia, E.A., Cislighi, A., Bischetti, G.B. & Comiti, F. (2020) Roots reinforcement by riparian trees in restored rivers. *Geomorphology*, 370, 107389. Available from: <https://doi.org/10.1016/j.geomorph.2020.107389>
- Beltaos, S. (2016) Extreme sediment pulses during ice breakup, Saint John River, Canada. *Cold Regions Science and Technology*, 128, 38–46. Available from: <https://doi.org/10.1016/j.coldregions.2016.05.005>
- Beltaos, S. & Burrell, B.C. (2010) Ice-jam model testing: Matapedia River case studies, 1994 and 1995. *Cold Regions Science and Technology*, 60(1), 29–39. Available from: <https://doi.org/10.1016/j.coldregions.2009.05.014>
- Beltaos, S. & Burrell, B.C. (2021) Effects of river-ice breakup on sediment transport and implications to stream environments: a review. *Water*, 13(18), 2541. Available from: <https://doi.org/10.3390/w13182541>
- Bertoldi, W. & Gurnell, A.M. (2020) Physical engineering of an island-braided river by two riparian tree species: evidence from aerial images and airborne lidar. *River Research and Applications*, rra.3657(7), 1183–1201. Available from: <https://doi.org/10.1002/rra.3657>
- Boivin, M., Buffin-Bélanger, T. & Piégay, H. (2017) Interannual kinetics (2010–2013) of large wood in a river corridor exposed to a 50-year flood event and fluvial ice dynamics. *Geomorphology, Dynamics and Ecology of Wood in World Rivers*, 279, 59–73. Available from: <https://doi.org/10.1016/j.geomorph.2016.07.010>
- Bollati, I.M., Pellegrini, L., Rinaldi, M., Duci, G. & Pelfini, M. (2014) Reach-scale morphological adjustments and stages of channel evolution: the case of the Trebbia River (northern Italy). *Geomorphology*, 221, 176–186. Available from: <https://doi.org/10.1016/j.geomorph.2014.06.007>
- Bornette, G., Tabacchi, E., Hupp, C., Puijalón, S. & Rostan, J.C. (2008) A model of plant strategies in fluvial hydrosystems. *Freshwater Biology*,

- 53(8), 1692–1705. Available from: <https://doi.org/10.1111/j.1365-2427.2008.01994.x>
- Boucher, É. (2017) River ice and ice jams. In: *International encyclopedia of geography*. Hoboken, NJ: John Wiley & Sons, Ltd, pp. 1–8. Available from: <https://doi.org/10.1002/9781118786352.wbieg0512>
- Boucher, É., Bégin, Y. & Arseneault, D. (2009) Impacts of recurring ice jams on channel geometry and geomorphology in a small high-boreal watershed. *Geomorphology*, 108(3–4), 273–281. Available from: <https://doi.org/10.1016/j.geomorph.2009.02.014>
- Boucher, E., Bégin, Y., Arseneault, D. & Ouarda, T.B.M.J. (2012) In: Church, M., Biron, P.M. & Roy, A.G. (Eds.) *Long-term and large-scale River-ice processes in cold-region watersheds*. Gravel-Bed Rivers: Wiley, pp. 546–554 <https://doi.org/10.1002/9781119952497.ch39>
- Buffin-Belanger, T., Beaudoin, J.-F., Maltais, M., Laroche, S., and Tomety, Y., (2022). Cartographie des zones inondables dans la MRC de Bonaventure. Volet 1 - Analyse et cartographie des aléas. Rapport remis au Ministère des Affaires municipales et de l'habitation, décembre 2022, 68 pages et annexes.
- Bywater-Reyes, S., Diehl, R.M., Wilcox, A.C., Stella, J.C. & Kui, L. (2022) A green new Balance: interactions among riparian vegetation plant traits and morphodynamics in alluvial rivers. *Earth Surface Processes and Landforms*, 47(10), 2410–2436. Available from: <https://doi.org/10.1002/esp.5385>
- Chassiot, L., Lajeunesse, P. & Bernier, J.-F. (2020) Riverbank erosion in cold environments: review and outlook. *Earth-Science Reviews*, 207, 103231. Available from: <https://doi.org/10.1016/j.earscirev.2020.103231>
- Chen, F., Chen, L., Zhang, W., Han, J. & Wang, J. (2019) Responses of channel morphology to flow-sediment variations after dam construction: a case study of the Shashi reach, middle Yangtze River. *Hydrology Research*, 50(5), 1359–1375. Available from: <https://doi.org/10.2166/nh.2019.066>
- Comiti, F., Cadol, D. & Wohl, E. (2009) Flow regimes, bed morphology, and flow resistance in self-formed step-pool channels. *Water Resources Research*, 45(4), W04424. Available from: <https://doi.org/10.1029/2008WR007259>
- Corenblit, D., Piégay, H., Arrignon, F., González-Sargas, E., Bonis, A., Davies, N.S., et al. (2024) Interactions between vegetation and river morphodynamics. Part I: research clarifications and challenges. *Earth-Science Reviews*, 253, 104769. Available from: <https://doi.org/10.1016/j.earscirev.2024.104769>
- Corenblit, D., Piégay, H., Arrignon, F., González-Sargas, E., Bonis, A., Ebengo, D.M., et al. (2024) Interactions between vegetation and river morphodynamics. Part II: why is a functional trait framework important? *Earth-Science Reviews*, 253, 104709. Available from: <https://doi.org/10.1016/j.earscirev.2024.104709>
- Corenblit, D., Steiger, J., Dufour, S., Liébault, F. & Piégay, H. (2024) Chapter 13 - Resilience and the biophysical science of rivers. In: Thoms, M. & Fuller, I. (Eds.) *Resilience and riverine landscapes*. Amsterdam, NL: Elsevier, pp. 269–286. Available from: <https://doi.org/10.1016/B978-0-323-91716-2.00010-8>
- Corenblit, D., Steiger, J., González, E., Gurnell, A.M., Charrier, G., Darrozes, J., et al. (2014) The biogeomorphological life cycle of poplars during the fluvial biogeomorphological succession: a special focus on *Populus nigra* L. *Earth Surface Processes and Landforms*, 39(4), 546–563. Available from: <https://doi.org/10.1002/esp.3515>
- Corenblit, D., Steiger, J. & Tabacchi, E. (2010) Biogeomorphologic succession dynamics in a Mediterranean river system. *Ecography*, 33(6), 1136–1148. Available from: <https://doi.org/10.1111/j.1600-0587.2010.05894.x>
- Corenblit, D., Tabacchi, E., Steiger, J. & Gurnell, A.M. (2007) Reciprocal interactions and adjustments between fluvial landforms and vegetation dynamics in river corridors: a review of complementary approaches. *Earth-Science Reviews*, 84(1–2), 56–86. Available from: <https://doi.org/10.1016/j.earscirev.2007.05.004>
- Corenblit, D., Vautier, F., González, E. & Steiger, J. (2020) Formation and dynamics of vegetated fluvial landforms follow the biogeomorphological succession model in a channelized river. *Earth Surface Processes and Landforms*, 45(9), 2020–2035. Available from: <https://doi.org/10.1002/esp.4863>
- De Munck, S., Gauthier, Y., Bernier, M., Chokmani, K. & Légaré, S. (2017) River predisposition to ice jams: a simplified geospatial model. *Natural Hazards and Earth System Sciences*, 17(7), 1033–1045. Available from: <https://doi.org/10.5194/nhess-17-1033-2017>
- Dufour, S., Barsoum, N., Muller, E. & Piégay, H. (2007) Effects of channel confinement on pioneer woody vegetation structure, composition and diversity along the river Drôme (SE France). *Earth Surface Processes and Landforms*, 32(8), 1244–1256. Available from: <https://doi.org/10.1002/esp.1556>
- Dumitriu, D. (2020) Sediment flux during flood events along the Trotuş River channel: hydrogeomorphological approach. *Journal of Soils and Sediments*, 20(11), 4083–4102. Available from: <https://doi.org/10.1007/s11368-020-02763-4>
- Edwards, P.J., Kollmann, J., Gurnell, A.M., Petts, G.E., Tockner, K. & Ward, J.V. (1999) A conceptual model of vegetation dynamics on gravel bars of a large Alpine river. *Wetlands Ecology and Management*, 7, 141–153. Available from: <https://doi.org/10.1023/A:1008411311774>
- Elder, B.D. (2003) The impact of changing flow regimes on riparian vegetation and the riparian species *Mimulus guttatus*. *Ecological Applications*, 13(6), 1610–1625. Available from: <https://doi.org/10.1890/02-5371>
- Engström, J., Jansson, R., Nilsson, C. & Weber, C. (2011) Effects of river ice on riparian vegetation: ice and riparian vegetation. *Freshwater Biology*, 56(6), 1095–1105. Available from: <https://doi.org/10.1111/j.1365-2427.2010.02553.x>
- Ettema, R. & Kempema, E.W. (2012) River-ice effects on gravel-bed channels. In: Church, M., Biron, P.M. & Roy, A.G. (Eds.) *Gravel-bed Rivers*. Hoboken, NJ: Wiley, pp. 523–540. Available from: <https://doi.org/10.1002/9781119952497.ch37>
- Fryirs, K.A. (2017) River sensitivity: a lost foundation concept in fluvial geomorphology: river sensitivity: a lost foundation concept in fluvial geomorphology. *Earth Surface Processes and Landforms*, 42(1), 55–70. Available from: <https://doi.org/10.1002/esp.3940>
- Garófano-Gómez, V., Arrignon, F., Vautier, F., Tabacchi, E., Allain, E., Bonis, A., et al. (2022) Trait-based numerical modelling of feedbacks between river morphodynamics and riparian vegetation for sustainable river management in a changing climate. In: *EGU general assembly 2022 conference abstracts*. Vienna, AT: European Geosciences Union, pp. EGU22-EGU7443. Available from: <https://doi.org/10.5194/egusphere-egu22-7443>
- Garófano-Gómez, V., Metz, M., Egger, G., Díaz-Redondo, M., Hortobágyi, B., Geerling, G., et al. (2017) Vegetation succession processes and fluvial dynamics of a mobile temperate riparian ecosystem: the lower Allier River (France). *Géomorphologie: Relief, Processus, Environnement*, 23(3), 187–202. Available from: <https://doi.org/10.4000/geomorphologie.11805>
- Geerling, G.W., Ragas, A.M.J., Leuven, R.S.E.W., van den Berg, J.H., Breedveld, M., Liefhebber, D., et al. (2006) Succession and rejuvenation in floodplains along the river Allier (France). *Hydrobiologia*, 565(1), 71–86. Available from: <https://doi.org/10.1007/s10750-005-1906-6>
- González, E., Shafroth, P.B., Lee, S.R., Leverich, G.T., Real De Asua, R., Sherry, R.A., et al. (2019) Short-term geomorphological and riparian vegetation responses to a 40-year flood on a braided, dryland river. *Ecohydrology*, 12(8), e2152. Available from: <https://doi.org/10.1002/eco.2152>
- Grams, P.E., Dean, D.J., Walker, A.E., Kasprak, A. & Schmidt, J.C. (2020) The roles of flood magnitude and duration in controlling channel width and complexity on the Green River in Canyonlands, Utah, USA. *Geomorphology*, 371, 107438. Available from: <https://doi.org/10.1016/j.geomorph.2020.107438>
- Gurnell, A.M. & Bertoldi, W. (2020) Extending the conceptual model of river island development to incorporate different tree species and environmental conditions. *River Research and Applications*, 36(8), 1730–1747. Available from: <https://doi.org/10.1002/rra.3691>
- Gurnell, A.M. & Bertoldi, W. (2024) Plants and river morphodynamics: the emergence of fluvial biogeomorphology. *River Research and Applications* n/a, 1–56(6), 887–942. Available from: <https://doi.org/10.1002/rra.4271>

- Han, M., Brierley, G., Li, B., Li, Z. & Li, X. (2020) Impacts of flow regulation on geomorphic adjustment and riparian vegetation succession along an anabranching reach of the upper Yellow River. *Catena*, 190, 104561. Available from: <https://doi.org/10.1016/j.catena.2020.104561>
- Jansson, R., Zinko, U., Merritt, D.M. & Nilsson, C. (2005) Hydrochory increases riparian plant species richness: a comparison between a free-flowing and a regulated river: *Hydrochory and plant species richness*. *Journal of Ecology*, 93(6), 1094–1103. Available from: <https://doi.org/10.1111/j.1365-2745.2005.01057.x>
- Jautzy, T., Schmitt, L. & Rixhon, G. (2022) Historical geomorphological adjustments of an upper Rhine sub-tributary over the two last centuries (Bruche River, France). *Géomorphologie: Relief, Processus, Environnement*, 28(1), 53–72. Available from: <https://doi.org/10.4000/geomorphologie.16661>
- Jones, L.S. & Schumm, S.A. (1999) Causes of Avulsion: An Overview. In: *Fluvial Sedimentology VI*. Hoboken, NJ: John Wiley & Sons, Ltd, pp. 169–178. Available from: <https://doi.org/10.1002/9781444304213.ch13>
- Karle, K.F. (2003) *Evaluation of bioengineered stream Bank stabilization in Alaska* (no. FHWA-AK-RD-03-03). Juneau, AK: Alaska Department of Transportation.
- Karle, K.F. (2007) *The effects of a winter ice jam event on bioengineered Bank stabilization along the Kenai River* (no. FHWA-AK-RD-07-03). Juneau, AK: Alaska Department of Transportation.
- Karrenberg, S., Edwards, P.J. & Kollmann, J. (2002) The life history of Salicaceae living in the active zone of floodplains. *Freshwater Biology*, 47(4), 733–748. Available from: <https://doi.org/10.1046/j.1365-2427.2002.00894.x>
- Kimiaghali, N., Goharrokhi, M., Clark, S.P. & Ahmari, H. (2015) A comprehensive fluvial geomorphology study of riverbank erosion on the Red River in Winnipeg, Manitoba, Canada. *Journal of Hydrology*, 529, 1488–1498. Available from: <https://doi.org/10.1016/j.jhydrol.2015.08.033>
- Kolerski, T. & Shen, H.T. (2015) Possible effects of the 1984 St. Clair River ice jam on bed changes. *Canadian Journal of Civil Engineering*, 42(9), 696–703. Available from: <https://doi.org/10.1139/cjce-2014-0275>
- Kovachis, N., Burrell, B.C., Huokuna, M., Beltaos, S., Turcotte, B. & Jasek, M. (2017) Ice-jam flood delineation: challenges and research needs. *Canadian Water Resources Journal/Revue Canadienne Des Ressources Hydriques*, 42(3), 258–268. Available from: <https://doi.org/10.1080/07011784.2017.1294998>
- Kramer, N. & Wohl, E. (2014) Estimating fluvial wood discharge using time-lapse photography with varying sampling intervals. *Earth Surface Processes and Landforms*, 39(6), 844–852. Available from: <https://doi.org/10.1002/esp.3540>
- Kyuka, T., Yamaguchi, S., Inoue, Y., Arnez Ferrel, K.R., Kon, H. & Shimizu, Y. (2021) Morphodynamic effects of vegetation life stage on experimental meandering channels. *Earth Surface Processes and Landforms*, esp.5051(7), 1225–1237. Available from: <https://doi.org/10.1002/esp.5051>
- Lallias-Tacon, S., Liébault, F. & Piégay, H. (2017) Use of airborne LiDAR and historical aerial photos for characterising the history of braided river floodplain morphology and vegetation responses. *CATENA, Geocology in Mediterranean mountain areas. Tribute to Professor José María García Ruiz*, 149, 742–759. Available from: <https://doi.org/10.1016/j.catena.2016.07.038>
- Lind, L. & Nilsson, C. (2015) Vegetation patterns in small boreal streams relate to ice and winter floods. *Journal of Ecology*, 103(2), 431–440. Available from: <https://doi.org/10.1111/1365-2745.12355>
- Lind, L., Nilsson, C., Polvi, L.E. & Weber, C. (2014) The role of ice dynamics in shaping vegetation in flowing waters: ice dynamics and vegetation in flowing waters. *Biological Reviews*, 89(4), 791–804. Available from: <https://doi.org/10.1111/brv.12077>
- Livingston, J.M., Smith, D.G., Froese, D.G. & Hugenholtz, C.H. (2009) Floodplain stratigraphy of the ice jam dominated middle Yukon River: a new approach to long-term flood frequency. *Hydrological Processes*, 23(3), 357–371. Available from: <https://doi.org/10.1002/hyp.7106>
- Lubiniecki, T., Laroque, C.P. & Lindenschmidt, K.-E. (2024) Identifying ice-jam flooding events through the application of dendrogeomorphological methods. *River Research and Applications*, 40(2), 191–202. Available from: <https://doi.org/10.1002/rra.4222>
- Lytle, D.A. & Poff, N.L. (2004) Adaptation to natural flow regimes. *Trends in Ecology & Evolution*, 19(2), 94–100. Available from: <https://doi.org/10.1016/j.tree.2003.10.002>
- Micheli, E.R., Kirchner, J.W. & Larsen, E.W. (2004) Quantifying the effect of riparian forest versus agricultural vegetation on river meander migration rates, Central Sacramento River, California, USA. *River Research and Applications*, 20(5), 537–548. Available from: <https://doi.org/10.1002/rra.756>
- Morin, S., Boucher, E. & Buffin-Belanger, T. (2015) The spatial variability of ice-jam bank morphologies along the Mistassini River (Quebec, Canada): an indicator of the ice-jam regime? *Natural Hazards*, 77(3), 2117–2138. Available from: <https://doi.org/10.1007/s11069-015-1693-y>
- Mossa, J., Chen, Y., Kondolf, G.M. & Walls, S.P. (2020) Channel and vegetation recovery from dredging of a large river in the Gulf coastal plain, USA. *Earth Surface Processes and Landforms*, 45(9), 1926–1944. Available from: <https://doi.org/10.1002/esp.4856>
- Ochs, K., Egger, G., Kopecki, I. & Ferreira, T. (2019) Model-based reconstruction of the succession dynamics of a large river floodplain. *River Research and Applications*, 35(7), 944–954. Available from: <https://doi.org/10.1002/rra.3502>
- Peters, D.L., Caissie, D., Monk, W.A., Rood, S.B. & St-Hilaire, A. (2016) An ecological perspective on floods in Canada. *Canadian Water Resources Journal/Revue Canadienne Des Ressources Hydriques*, 41(1-2), 288–306. Available from: <https://doi.org/10.1080/07011784.2015.1070694>
- Poulin, M., Evette, A., Tisserant, M., Keita, N., Breton, V., Biron, P., et al. (2019) Le génie végétal pour la protection des berges de cours d'eau au Québec: état des lieux et perspectives pour les Basses-terres du Saint-Laurent. *Sciences Eaux & Territoires*, 57, 7. Available from: <https://doi.org/10.14758/SET-REVUE.2019.HS.06>
- Prowse, T.D. & Culp, J.M. (2003) Ice breakup: a neglected factor in river ecology. *Canadian Journal of Civil Engineering*, 30(1), 17–144. Available from: <https://doi.org/10.1139/I02-040>
- Rood, S.B., Goater, L.A., Mahoney, J.M., Pearce, C.M. & Smith, D.G. (2007) Floods, fire, and ice: disturbance ecology of riparian cottonwoods. *Canadian Journal of Botany*, 85(11), 1019–1032. Available from: <https://doi.org/10.1139/B07-073>
- Scorpio, V. & Comiti, F. (2024) Channel changes during and after extreme floods in two catchments of the northern Apennines (Italy). *Geomorphology*, 463, 109355. Available from: <https://doi.org/10.1016/j.geomorph.2024.109355>
- Segura-Beltrán, F. & Sanchis-Ibor, C. (2013) Assessment of channel changes in a Mediterranean ephemeral stream since the early twentieth century. The Rambla de Cervera, eastern Spain. *Geomorphology*, 201, 199–214. Available from: <https://doi.org/10.1016/j.geomorph.2013.06.021>
- Serlet, A.J., Gurnell, A.M., Zolezzi, G., Wharton, G., Belleudy, P. & Jourdain, C. (2018) Biomorphodynamics of alternate bars in a channelized, regulated river: an integrated historical and modelling analysis: BIOMORPHODYNAMICS OF ALTERNATE BARS IN A CHANNELIZED, REGULATED RIVER. *Earth Surface Processes and Landforms*, 43(9), 1739–1756. Available from: <https://doi.org/10.1002/esp.4349>
- Smith, D.G. & Pearce, C.M. (2000) River ice and its role in limiting woodland development on a sandy braid-plain, Milk River, Montana. *Wetlands*, 20(2), 232–250. Available from: [https://doi.org/10.1672/0277-5212\(2000\)020\[0232:RIAIRJ\]2.0.CO;2](https://doi.org/10.1672/0277-5212(2000)020[0232:RIAIRJ]2.0.CO;2)
- Smith, D.G. & Pearce, C.M. (2002) Ice jam-caused fluvial gullies and scour holes on northern river flood plains. *Geomorphology*, 42(1-2), 85–95. Available from: [https://doi.org/10.1016/S0169-555X\(01\)00076-9](https://doi.org/10.1016/S0169-555X(01)00076-9)
- Smith, N.D., Cross, T.A., Dufficy, J.P. & Clough, S.R. (1989) Anatomy of an avulsion. *Sedimentology*, 36(1), 1–23. Available from: <https://doi.org/10.1111/j.1365-3091.1989.tb00817.x>
- Steinberg, K.A., Eichhorst, K.D. & Rudgers, J.A. (2021) Flood regime alters the abiotic correlates of riparian vegetation. *Applied Vegetation Science*, 24(2), e12572. Available from: <https://doi.org/10.1111/avsc.12572>

- Surian, N., Barban, M., Ziliani, L., Monegato, G., Bertoldi, W. & Comiti, F. (2015) Vegetation turnover in a braided river: frequency and effectiveness of floods of different magnitude: VEGETATION TURN-OVER IN a BRAIDED RIVER. *Earth Surface Processes and Landforms*, 40(4), 542–558. Available from: <https://doi.org/10.1002/esp.3660>
- Tal, M. & Paola, C. (2010) Effects of vegetation on channel morphodynamics: results and insights from laboratory experiments. *Earth Surface Processes and Landforms*, 35(9), 1014–1028. Available from: <https://doi.org/10.1002/esp.1908>
- Taylor, S.M., (2009). On the use of dendrochronology to analyse ice jam occurrences at a fluvial transition on the Ouelle River, Quebec.
- Turcotte, B., Morse, B., Bergeron, N.E. & Roy, A.G. (2011) Sediment transport in ice-affected rivers. *Journal of Hydrology*, 409(1-2), 561–577. Available from: <https://doi.org/10.1016/j.jhydrol.2011.08.009>
- Uunila, L. & Church, M. (2014) Ice on Peace River: Effects on Bank Morphology and Riparian Vegetation. In: Church, M. (Ed.) *The regulation of Peace River*. Chichester, UK: John Wiley & Sons, Ltd, pp. 115–140 <https://doi.org/10.1002/9781118906170.ch6>
- Vandermause, R., Harvey, M., Zevenbergen, L. & Ettema, R. (2021) River-ice effects on bank erosion along the middle segment of the Susitna river, Alaska. *Cold Regions Science and Technology*, 185, 103239. Available from: <https://doi.org/10.1016/j.coldregions.2021.103239>
- Yang, S., Bai, Y. & Xu, H. (2018) Experimental analysis of river evolution with riparian vegetation. *Water*, 10(11), 1500. Available from: <https://doi.org/10.3390/w10111500>
- Yu, G.-A., Li, Z., Yang, H., Lu, J., Huang, H.Q. & Yi, Y. (2020) Effects of riparian plant roots on the unconsolidated bank stability of meandering channels in the Tarim River, China. *Geomorphology*, 351, 106958. Available from: <https://doi.org/10.1016/j.geomorph.2019.106958>
- Yumoto, M., Ogata, T., Matsuoka, N. & Matsumoto, E. (2006) Riverbank freeze-thaw erosion along a small mountain stream, Nikko volcanic area, Central Japan. *Permafrost and Periglacial Processes*, 17(4), 325–339. Available from: <https://doi.org/10.1002/ppp.569>

## SUPPORTING INFORMATION

Additional supporting information can be found online in the Supporting Information section at the end of this article.

**How to cite this article:** Prugne, M., Corenblit, D., Boivin, M. & Buffin-Bélanger, T. (2025) Vegetation and channel adjustment trajectories in cold regions: The effects of ice disturbances in two Gaspesian rivers. *Earth Surface Processes and Landforms*, 50(5), e70051. Available from: <https://doi.org/10.1002/esp.70051>